PALEOCLIMA

Scala temporale degli isotopi dell'ossigeno

L'ossigeno ha tre isotopi stabili: ^{16}O, ^{17}O e ^{18}O.

I materiali naturali contengono circa lo 0.2 % di ossigeno 18.

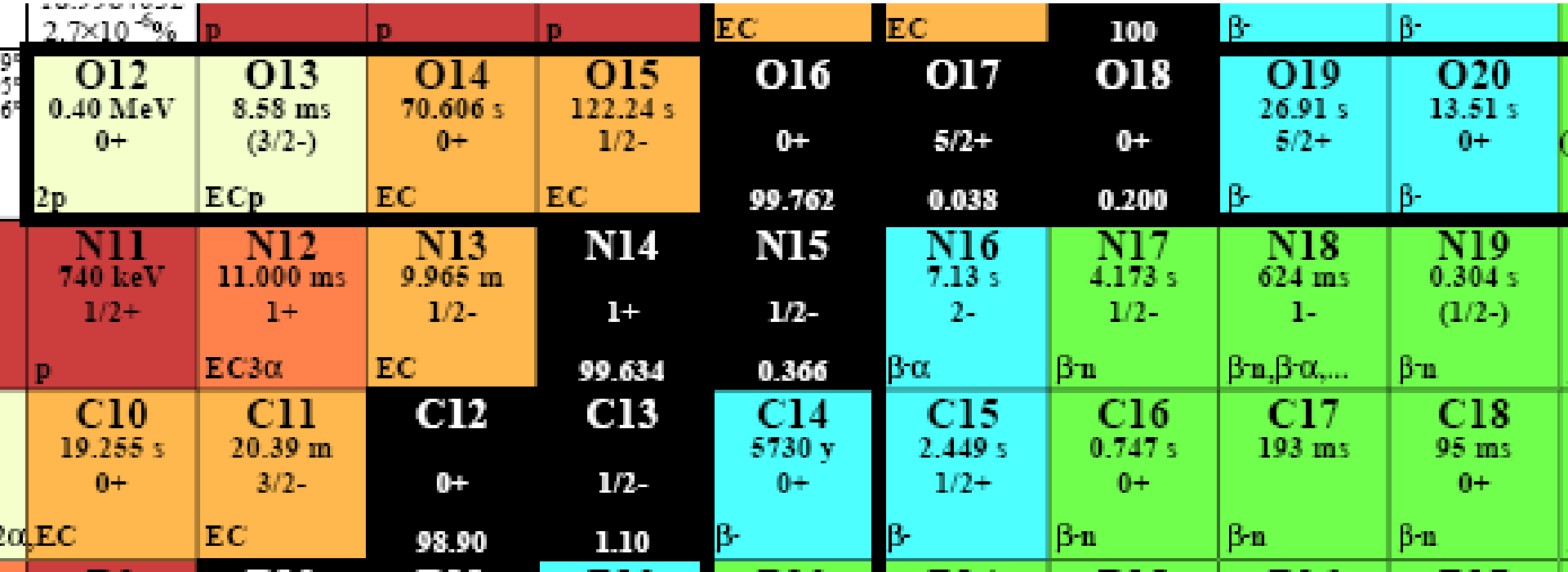

C’è un frazionamento isotopico piccolo, ma misurabile con precisione tramite uno spettrometro di massa. Il frazionamento dipende dalla temperatura e quindi dà informazioni sul clima. Nei ghiacci il rapporto O18/O16 è minore che nell’acqua marina. La conseguenza più importante è che nei periodi glaciali i ghiacciai assorbono con leggera preferenza l’O16, che risulta quindi meno concentrato nell’acqua marina e negli organismi che fissano l’ossigeno. Il carbonato di calcio delle conchiglie marine contiene quindi meno ossigeno 16 nei periodi freddi.

C’è un secondo effetto, meno importante, che si somma collo stesso segno:

più bassa è la temperatura dell’acqua marina, meno O16 si trova nelle conchiglie.

Quindi, l’ ^{16}O è meno abbondante nelle conchiglie formatesi nei periodi più freddi per due motivi:

1) Ce n’è di meno nell’acqua marina

2) E’ sfavorito dal frazionamento isotopico

In un primo tempo si pensava che la causa fosse la seconda, ma poi si è scoperto che la prima domina largamente.

CLIMA GLOBALE

La tecnica consiste nel prelevare una carota con un diametro di circa 10 cm e lunga 10 m o più da un fondale oceanico profondo. Il deposito cresce di qualche cm per millennio ed è una mistura di sedimento terrigeno e infiltrazioni biogeniche formate da scheletri silicei (radiolaria, zooplancton e alghe) e calcarei (foraminifera, coccoliti) di origine superficiale (plancton) o profonda (bentica).

I prelievi sono effettuati anche dai ghiacci antartici, o da depositi continentali di loess. Nella Cina centrale c'è un deposito di un centinaio di metri che fornisce un registro completo dei cambi climatici per tutto il quaternario. Nei periodi caldi (interglaciali) si ha formazione di suolo, mentre nei periodi glaciali si hanno sedimenti portati dal vento o rilasciati dall'attrito del ghiacciaio con le rocce. In genere c'è un marcato segno del passaggio tra i due tipi di deposito dei periodi caldi e freddi.

Oltre che sulla tecnica di misura della concentrazione degli isotopi di ossigeno, la datazione si può basare su misura magnetiche (il deposito terrigeno ha una debole suscettività magnetica) o su tecniche di luminescenza.

Un’altra forma di registro completo si ha da occasionali lunghe sequenze di pollini che vanno indietro fino all’inizio dell’ultimo periodo interglaciale o anche a periodi precedenti in alcuni casi.

Oltre al rapporto tra gli isotopi di ossigeno, si misurano altre cose. Nelle carote di ghiaccio antartico, il rapporto tra deuterio e idrogeno, la quantità di anidride carbonica catturata nella porosità del ghiaccio, il rapporto tra isotopi del carbonio, il rapporto tra osigeno ed azoto ….

Nel caso della misura del rapporto tra gli isotopi di ossigeno, la quantità che si usa riportare è

$$\delta\,^{18}O = \frac{(^{18}O/^{16}O)_{sample} - (^{18}O/^{16}O)_{standard}}{(^{18}O/^{16}O)_{standard}} \times 1000$$

cioè l’eccesso di ossigeno 18 rispetto allo standard, misurato in per mille.

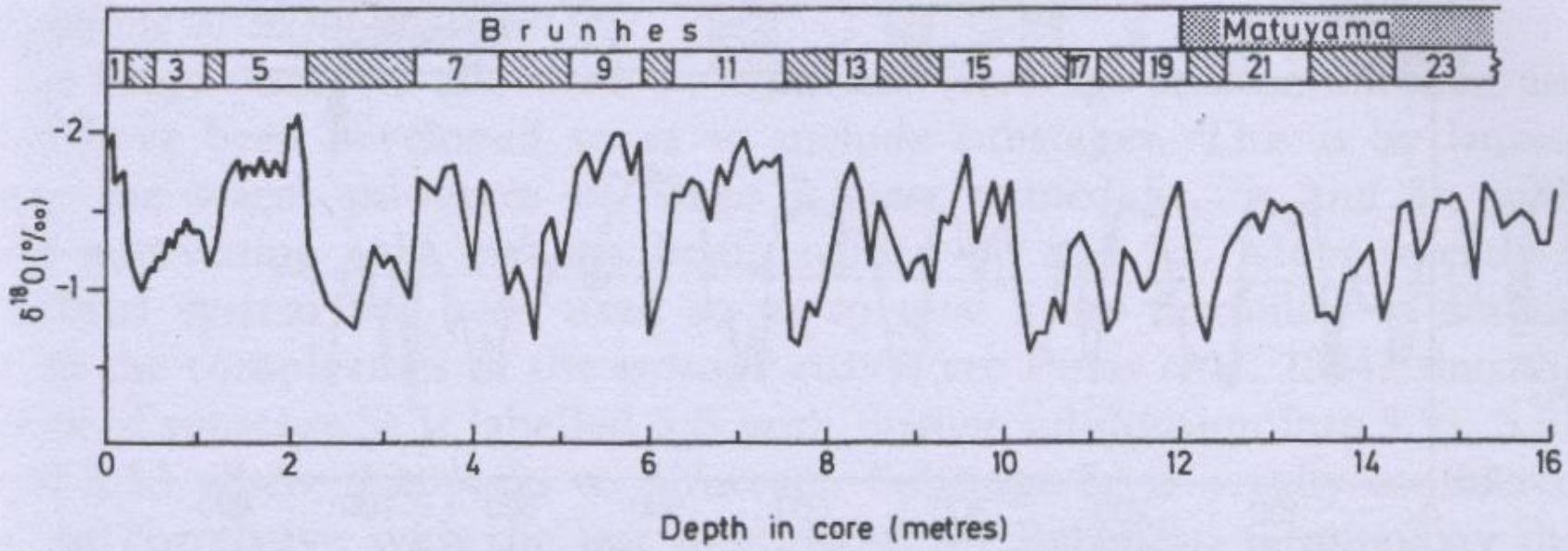

Fig. 2.3 Oxygen–isotope variation in core V28–238 from the Pacific (Shackleton and Opdyke 1973, 1976). During the isotope stage 19 the magnetization of the sediment changed from reverse polarity (Matuyama chron) to normal polarity (Brunhes chron); the accepted age for this change was 700,000 years at the time the core was measured (subsequently revised to 730,000 years). The time-scale for the isotope variations was obtained by using this age and assuming a constant sedimentation rate, with radiocarbon dating for the upper part of the core (redrawn from Shackleton and Opdyke 1973).

Ricordando che negli oceani ia concentrazione di ossigeno 18 aumenta rispetto a quella di ossigeno 17 e ossigeno 16 nei periodi freddi, la scala delle ordinate indica caldo in alto e freddo in basso.

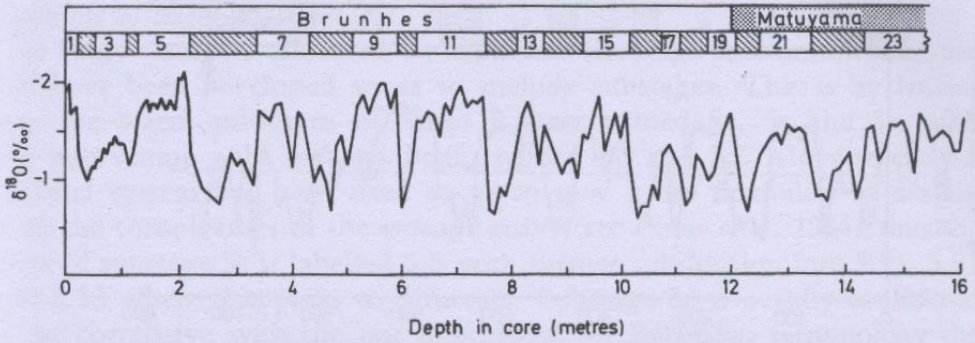

Fig. 2.3 Oxygen–isotope variation in core V28–238 from the Pacific (Shackleton and Opdyke 1973, 1976). During the isotope stage 19 the magnetization of the sediment changed from reverse polarity (Matuyama chron) to normal polarity (Brunhes chron); the accepted age for this change was 700,000 years at the time the core was measured (subsequently revised to 730,000 years). The time-scale for the isotope variations was obtained by using this age and assuming a constant sedimentation rate, with radiocarbon dating for the upper part of the core (redrawn from Shackleton and Opdyke 1973).

Problemi più importanti:

1) Trasformare la scala in ascissa in una scala temporale
2) Trasformare la scala in ordinata in una scala di temperatura
3) Sincronizzare tra loro le varie misure locali e capire cosa è globale e cosa non lo è.
4) Collegare i periodi climatici allo sviluppo della vita degli uomini e ominidi che li hanno preceduti

1) Si è usato sempre tutto quanto era disponibile: in un primo tempo C14 per le fasi più recenti, l'inversione magnetica, datata con metodi nucleari a circa 700.000 anni fa (valore attuale più probabile 776 ± 12 ka) e osservabile nello stadio 19 (Matuyama chron) e l'ipotesi di lavoro di un ritmo di sedimentazione costante. Ora la scala è basata su una teoria astronomica che fornisce l'età di ogni fase con estrema precisione.

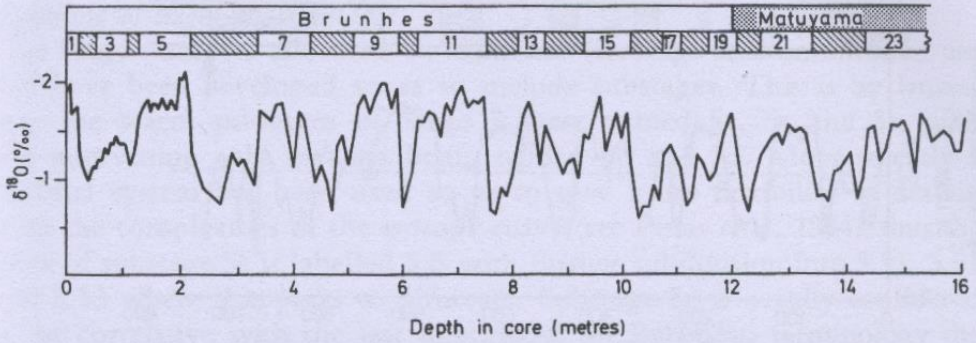

Fig. 2.3 Oxygen–isotope variation in core V28–238 from the Pacific (Shackleton and Opdyke 1973, 1976). During the isotope stage 19 the magnetization of the sediment changed from reverse polarity (Matuyama chron) to normal polarity (Brunhes chron); the accepted age for this change was 700,000 years at the time the core was measured (subsequently revised to 730,000 years). The time-scale for the isotope variations was obtained by using this age and assuming a constant sedimentation rate, with radiocarbon dating for the upper part of the core (redrawn from Shackleton and Opdyke 1973).

Problemi più importanti:

1) Trasformare la scala in ascissa in una scala temporale
2) Trasformare la scala in ordinata in una scala di temperatura
3) Sincronizzare tra loro le varie misure locali e capire cosa è globale e cosa non lo è.
4) Collegare i periodi climatici allo sviluppo della vita degli uomini e ominidi che li hanno preceduti

1) La scala in alto, che riporta fasi numerate con numeri dispari ha a che fare sia con il problema 1, che con il 2 ed il 3. Le fasi dispari corrispondono a periodi interglaciali, quelle pari, non riportate a periodi glaciali. Una tale classificazione è rozza perché si intuisce anche dalla figura che c'è una struttura fine con periodi più caldi in una fase glaciale (interstadiali) e periodi più freddi in una interglaciale (stadiali), che ora si usa indicare utilizzando un secondo o anche un terzo indice (per es. 5.53). Una caratteristica importante è la rapida variazione climatica avvenuta alla fine di molte ere glaciali.

TERMINOLOGIA DELLE PRINCIPALI EPOCHE CLIMATICHE

Negli ultimi 2 Myr (quaternario) si sono succedute una ventina di fasi glaciali e interglaciali. Il passaggio dal Pliocene, l'ultimo periodo del Terziario, al Pleistocene, il primo del quaternario è stato caratterizzato da un improvviso calo della temperatura, anche se c'è evidenza di qualche glaciazione nell'ultimo periodo del Pliocene.

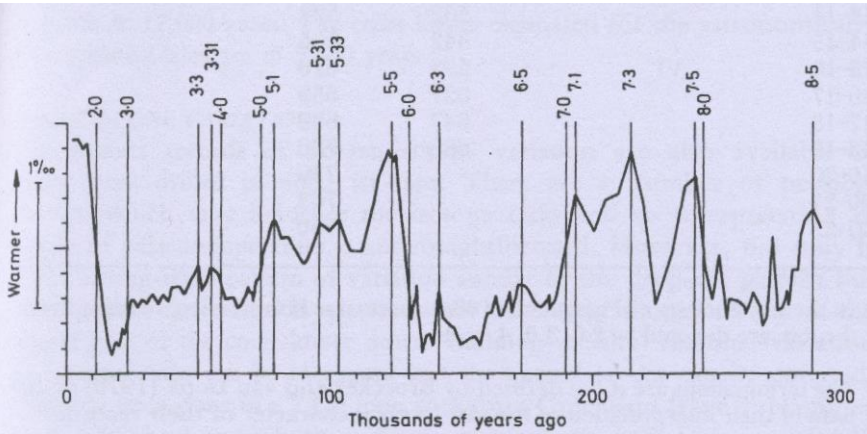

Fig. 2.8 High-resolution oxygen–isotope variation for the past 300,000 years with time-scale based on orbital tuning (redrawn from Martinson *et al.* 1987). The curve is the averaged record from five deep-sea cores from various oceans of the world, but using benthic (bottom-dwelling) foraminifera instead of the planktonic (surface-dwelling) foraminifera that were used for Fig. 2.7; the core locations were different, too. Dates for stage boundaries (2.0, 3.0, 4,0, etc.) are included in Table 2.4.

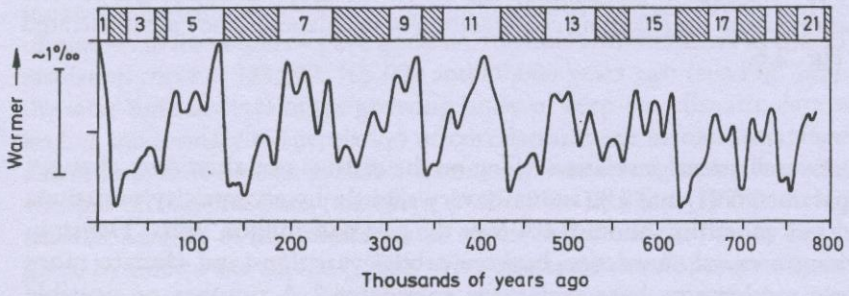

Fig. 2.7 Oxygen–isotope variations for the past 800,000 years with time-scale based on orbital tuning (redrawn from Imbrie *et al.* 1984). The curve is the smoothed record obtained from planktonic foraminifera of five deep-sea cores distributed around the oceans of the world. The numbers along the top indicate warm stages; dates for stage boundaries are included in Table 2.4. The vertical scale is in normalized units such that the standard deviation of the curve is equal to 1 unit.

La nostra epoca, l'Olocene o post-glaciale, inizia circa 10.000 anni fa alla fine dell'ultima glaciazione. Il precedente periodo (3, Riss-Würm) classificato come interglaciale, tra circa 60.000 e 20.000 anni fa, era ben più freddo del nostro e del periodo 5 (Mindel-Riss, tra circa 130.000 e 75.000 anni fa).

Table 2.1 Some terminologies used in the northern hemisphere for glacial and interglacial [a] stages of the Quaternary

European Alps	*Northern Europe*[b]	*Britain*	*Central North America*	*China*[c]
Postglacial	*Holocene*	*Flandrian*	*Holocene*	*Postglacial*
Würm	Weichselian	Devensian	Wisconsinan	Dali
Riss-Würm	*Eemian*	*Ipswichian*	*Sangamon*	*Lushan-Dali*
Riss	Saalian	Wolstonian (?)	Illinoian	Lushan
Mindel-Riss	*Holsteinian*	*Hoxnian*	*Yarmouthian*	—
Mindel	Elsterian	Anglian	Kansan	Da Gu
Günz-Mindel	*Cromerian*	*Cromerian*	*Aftonian*	—
Günz	Menapian	Beestonian	Nebraskan	Poyang
Donau	*Waalian*	*Pastonian*		
Biber	Eburonian	Pre-Pastonian		
	Tiglian	*Bramertonian*		
	Pretiglian	Baventian		
		Antian		
		Thurnian		
		Ludhamian		
	Reuverian	Reuverian		

[a] Interglacials are shown in italics. Except for China this table is derived from Lowe and Walker (1984) who warn against assuming correlation between columns except in respect of the first two lines.

Pur se è stata osservata una correlazione precisa tra periodi freddi o caldi a livello globale, tuttavia sono state osservate importanti fluttuazioni locali che hanno portato a una complicazione nella classificazione. Per esempio, alcuni periodi considerati come interglaciali in molte regioni, in altre non hanno avuto queste grandi innalzamenti di temperatura e sono caratterizzabili solo come interstadiali.

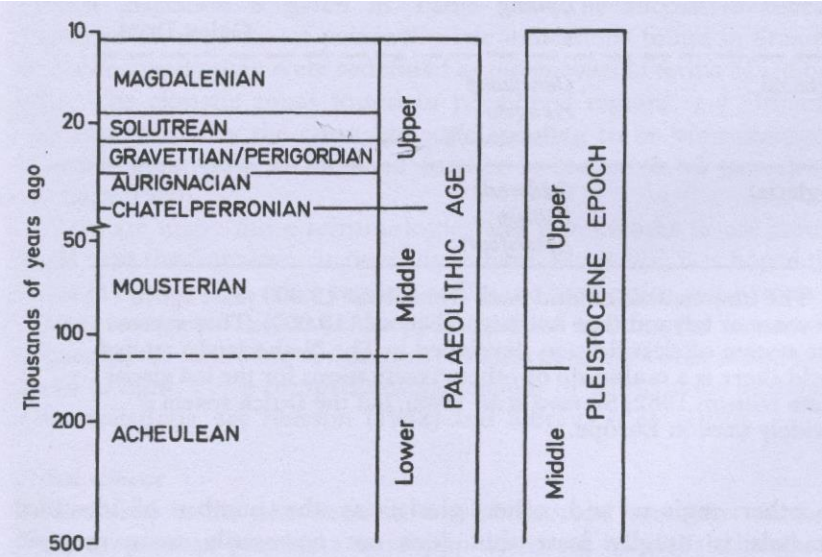

Fig. 2.1 Some archaeological subdivisions of the Palaeolithic lying within the Middle and Upper Pleistocene. Although the names derive from sites in Europe (as also the age scale), they tend to be used for similar cultural assemblages elsewhere.

La figura mostra alcuni termini usati per descrivere l'archeologia del Pleistocene Medio e Superiore (problema di correlare le epoche climatiche a quelle dello sviluppo umano e delle relative tecnologie degli strumenti in pietra). Una correlazione precisa tra le diverse regioni si ha solo per le prime due righe in alto.

Table 2.3 Subdivisions[a] of the Late-glacial and Postglacial phases of NW Europe

			Chronozone	*Radiocarbon years[b] before present*	*Calendar years[c] BC*
Postglacial	Holocene (Flandrian)	Late	Sub–Atlantic	2,500	550–800
		Middle	Sub–Boreal	5,000	3,800
			Atlantic	8,000	*c.*7,000
		Early	Boreal	9,000	*c.*8,000
			Pre–Boreal	10,000	*c.*9,000
Late-glacial		Late Weichselian	Younger Dryas	11,000	*c.*10,000
			Allerød	11,800	
			Older Dryas	12,000	
			Bølling	13,000	*c.*12,000

[a] The terminology for the Holocene is that proposed by Blytt and Sernarder on the basis of plant remains in Scandinavian peat bogs. Climatic descriptions: Pre-Boreal: Sub-Arctic; Boreal: warmer and dry; Atlantic: warm and wet; Sub-Boreal: warm and dry; Sub-Atlantic: cool and wet. The climatic optimum was reached at the boundary of the Atlantic and Sub-Boreal.

[b] The ages, in conventional radiocarbon years, are those used by Mangerud *et al.* (1974) to define chronozones (see section 2.4.3) which in the Holocene approximate to the Blytt and Sernarder climatic zones. In the Late Weichselian the Allerød and Bølling are interstadials (warm); the Bølling chronozone comprises both the Bølling interstadial and the Oldest Dryas cold zone preceding it. For a review of these phases see Turner and Hannon (1988).

[c] Calendar years BC are derived as indicated in section 4.4; beyond 7000 BC they are tentative.

CORRELAZIONI TRA DATI DI DIVERSE REGIONI E DATI OTTENUTI CON DIVERSE TECNICHE

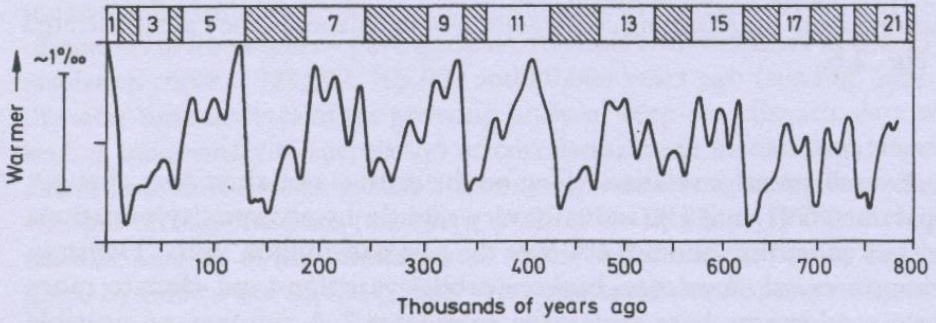

Fig. 2.7 Oxygen–isotope variations for the past 800,000 years with time-scale based on orbital tuning (redrawn from Imbrie *et al.* 1984). The curve is the smoothed record obtained from planktonic foraminifera of five deep-sea cores distributed around the oceans of the world. The numbers along the top indicate warm stages; dates for stage boundaries are included in Table 2.4. The vertical scale is in normalized units such that the standard deviation of the curve is equal to 1 unit.

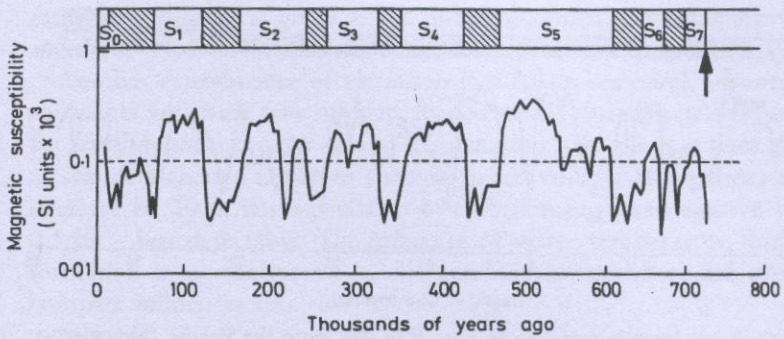

Fig. 2.4 Magnetic susceptibility profile in Chinese loess at Xifeng; also shown is the alternation of loess layers and palaeosols (S_0, S_1, S_2, etc.), corresponding to cold and warm periods respectively. For various reasons (see section 9.3.3) palaeosols have an enhanced magnetic susceptibility and this latter gives a more detailed record of climate than is otherwise available, high susceptibility being indicative of warmth (see Heller and Liu 1982, 1984, 1986). The pattern of variation synchronizes well with that of the deep-sea oxygen isotope but this is not necessarily true of other land regions (see, for example, Winograd *et al.* 1988).

The age scale has been derived by interpolation between the Brunhes–Matuyama magnetic polarity boundary (indicated by arrow) and the Holocene soil, S_0, dated by radiocarbon; the interpolation is on the basis that whereas the rate of loess deposition was uniform the time interval represented by a palaeosol layer was greater than that corresponding to its thickness by a factor dependent on magnetic susceptibility (Kukla *et al.* 1988). The above diagram, which is redrawn from Kukla (1987) is based on magnetic data by Liu *et al.* (1985). Magnetic susceptibility variations in loess profiles have also been reported from Alaska but in these the palaeosols are characterized by low values (Begét and Hawkins, 1989).

1) metodo: isotopi di ossigeno — suscettività magnetica
2) Origine: media oceanica mondiale — Cina centrale: loess
3) Scala temporale astronomica — Interpolazione dall' ultima inversione di H

Dai primi lavori pionieristici degli anni ‘50 del secolo scorso, le tecniche di indagine hanno avuto uno sviluppo eccezionale e la quantità di dati da elaborare e incrociare tra loro per ricostruire la storia del clima della terra sta aumentando di anno in anno.
In particolare, come vedremo, I carotaggi del ghiaccio antartico permettono di misurare:

- i rapporti isotopici dell’ossigeno e dell’idrogeno del ghiaccio
- Le quantità di gas inclusi nelle porosità. Importanti sono la CO_2 e CH_4 per la loro influenza sul riscaldamento globale (effetto serra), il rapporto N2/O2 che dà il clima locale e permette una preciso aggancio alle oscillazioni dell’insolazione estiva.
- Inclusioni di ogni tipo: in particolare ceneri vulcaniche,
- Contaminazioni varie. In partcolare la concentrazione di ^{10}Be, che fa parte di raggi cosmici, ha massimi in corrispondenza dei minimi del valore del campo magnetico terrestre e fornisce la datazione delle inversioni del campo.

Un semplice sguardo al numero degli autori delle pubblicazioni sul tema ci fa capire il crescendo di complessità e multidisciplinarietà di questo tipo di ricerche.

Cesare Emiliani, **Pleistocene Temperature, The Journal of Geology,** 63, 6, 1955
Oxygen isotopic analyses of pelagic Foraminifera from Atlantic, Caribbean, and Pacific deep-sea cores indicate that the temperature of superficial waters in the equatorial Atlantic and Caribbean underwent periodic oscillations during the Pleistocene with an amplitude of about 6° C. …..

NICHOLAS SHACKLETON, **Oxygen Isotope Analyses and Pleistocene Temperatures Re-assessed,** *Nature* **215**, 15 - 17 (1967).
Oxygen isotope analyses of foraminiferal tests in deep-sea cores have been interpreted as showing that the temperature of seawater in the Caribbean and equatorial Atlantic varied by as much as 6° C during glacial cycles. This evidence has now been reinterpreted, and changes in oxygen isotope composition are now said to correspond with the extraction of large amounts of water from the oceans during glacial periods and the recirculation of this water during periods when glaciers were at their present levels.

Clim. Past, 3, 485–497, 2007
www.clim-past.net/3/485/2007/

Climate of the Past

The EDC3 chronology for the EPICA Dome C ice core

F. Parrenin[1], J.-M. Barnola[1], J. Beer[2], T. Blunier[3], E. Castellano[4], J. Chappellaz[1], G. Dreyfus[5], H. Fischer[6], S. Fujita[7], J. Jouzel[5], K. Kawamura[8], B. Lemieux-Dudon[1], L. Loulergue[1], V. Masson-Delmotte[5], B. Narcisi[9], J.-R. Petit[1], G. Raisbeck[10], D. Raynaud[1], U. Ruth[6], J. Schwander[3], M. Severi[4], R. Spahni[3], J. P. Steffensen[11], A. Svensson[11], R. Udisti[4], C. Waelbroeck[1], and E. Wolff[12]

[1]Laboratoire de Glaciologie et Géophysique de l'Environnement, CNRS and Joseph Fourier University, Grenoble, France
[2]Department of Surface Waters, EAWAG, Dübendorf, Switzerland
[3]Climate and Environmental Physics, Physics Institute, University of Bern, Bern, Switzerland
[4]Department of Chemistry, University of Florence, Florence, Italy
[5]Laboratoire des Sciences du Climat et de l'Environnement, IPSL/CEA/CNRS/UVSQ, Gif-Sur-Yvette, France
[6]Alfred-Wegener-Institute for Polar and Marine Research, Bremerhaven, Germany
[7]National Institute of Polar Research, Research Organization of Information and Systems (ROIS), Tokyo, Japan
[8]Center for Atmospheric and Oceanic Studies Graduate School of Science, Tohoku University, Sendai, Japan
[9]ENEA, C. R. Casaccia, Roma, Italy
[10]CSNSM/IN2P3/CNRS, Orsay, France
[11]Niels Bohr Institute, University of Copenhagen, Copenhagen, Denmark
[12]British Antarctic Survey, Cambridge, UK

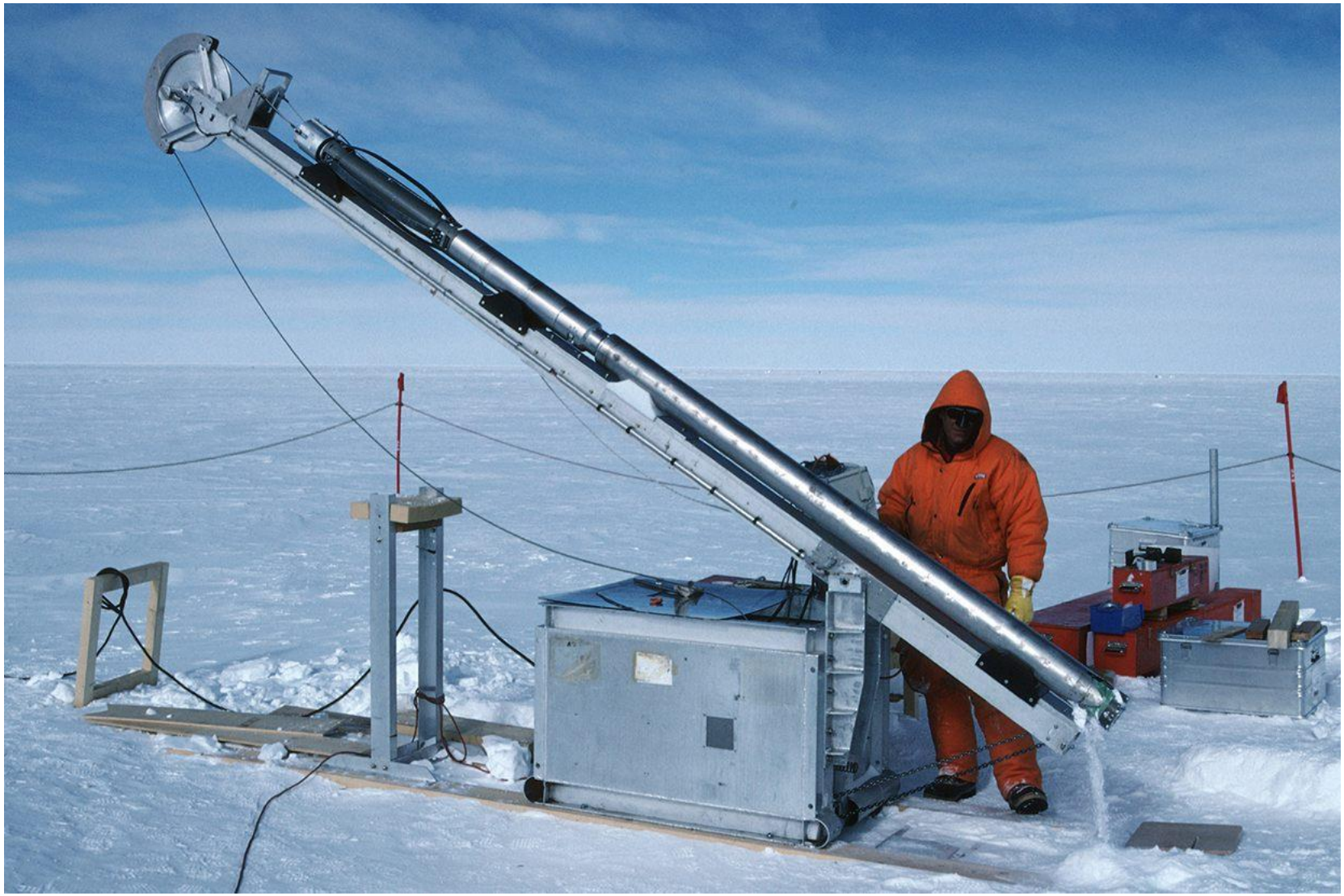

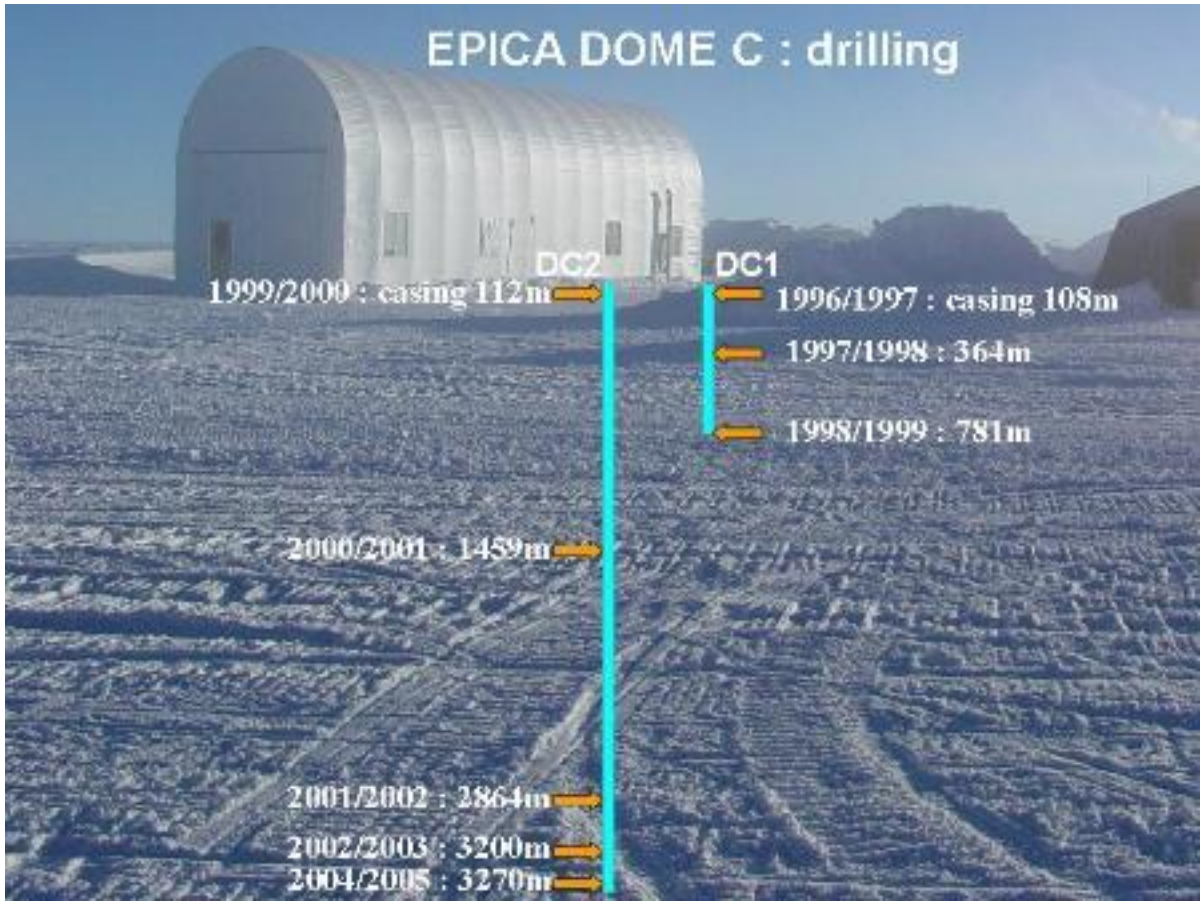

Concordia Station, Dome C (coordinates 75°06'S; 123°21'E, 3233 m above sea level).

This site was chosen to obtain the longest undisturbed chronicle of environmental change, in order to characterise climate variability over several glacial cycles, and to study potential climate forcings and their relationship to events in other regions. Drilling was completed at this site in December 2004, reaching a drilling depth of 3270.2 m, 5 m above bedrock. The retrieved core will extend the record to an age estimated to be around 890 000 years old.

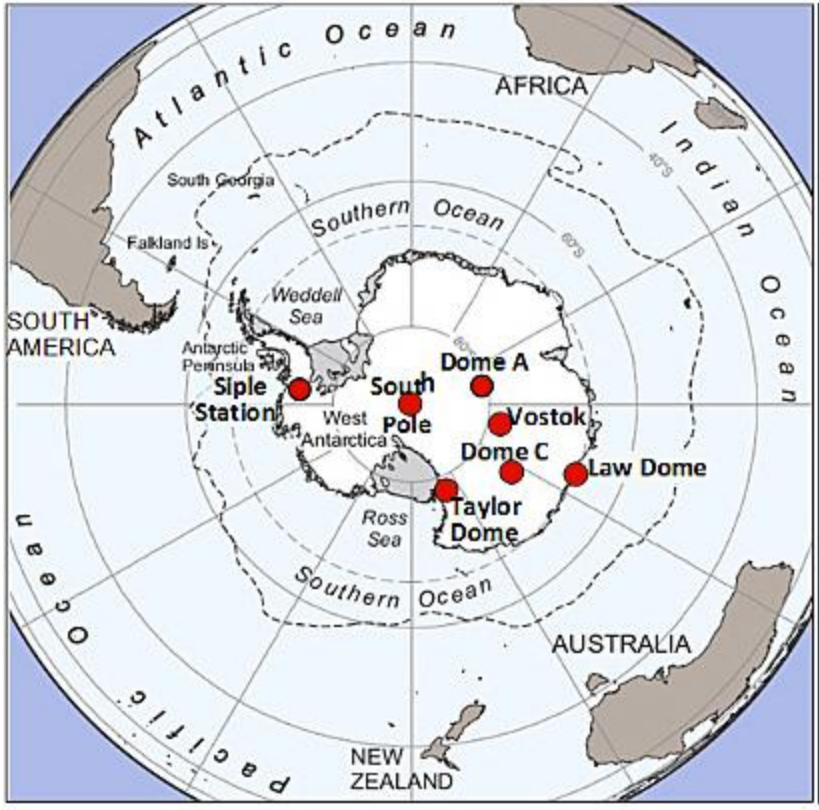
Atlantic Ocean
AFRICA
Indian Ocean
South Georgia
Falkland Is
Southern Ocean
Weddell Sea
SOUTH AMERICA
Antarctic Peninsula
Siple Station
South Pole
Dome A
Vostok
West Antarctica
Dome C
Law Dome
Taylor Dome
Ross Sea
Southern Ocean
AUSTRALIA
Pacific Ocean
NEW ZEALAND

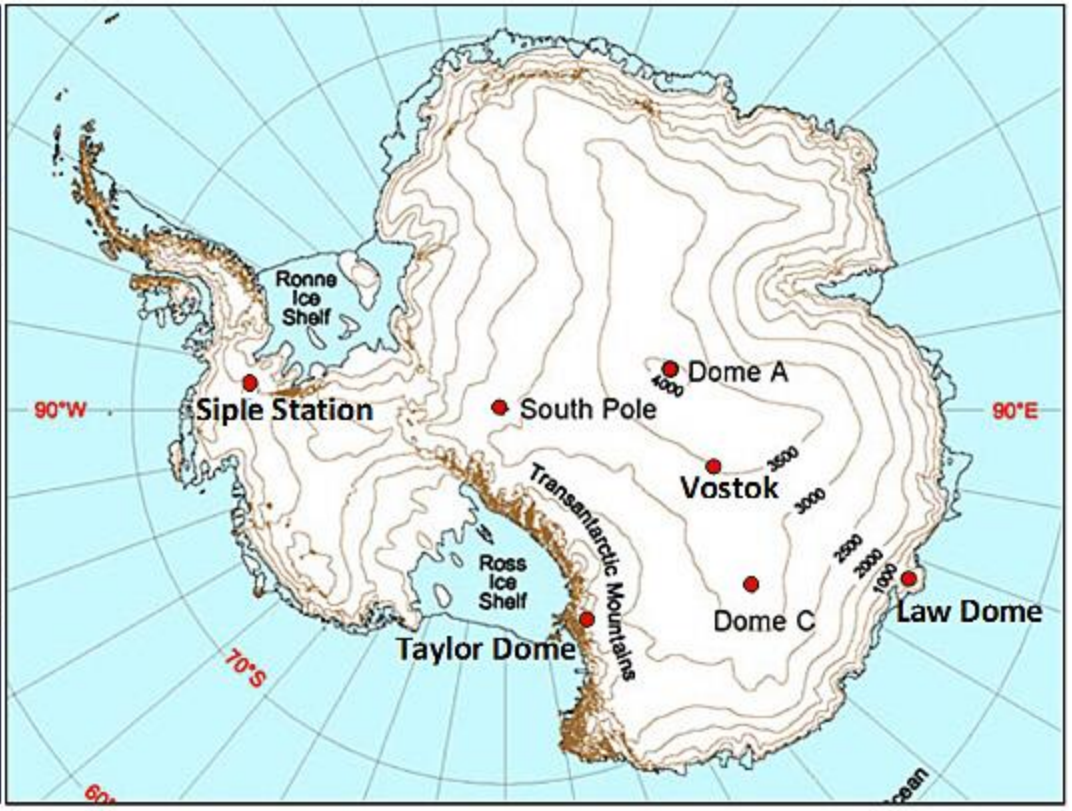
Ronne Ice Shelf
Siple Station
South Pole
Dome A
90°W
90°E
Vostok
Transantarctic Mountains
Ross Ice Shelf
Dome C
Law Dome
Taylor Dome
70°S

LA TEORIA ASTRONOMICA DEL CLIMA (MILANKOVITCH)

Il livello di insolazione non è costante nel tempo, ma varia periodicamente in intensità e distribuzione geografica e stagionale.

Ipotesi formulata nel 1920 e meglio formalizzata nel 1941 con la pubblicazione delle curve di insolazione a diverse latitudine per gli ultimi 600.000 anni.

Dopo diverse vicissitudini, fra cui il disaccordo con le prime datazioni (non calibrate) al C14 negli anni 50, il preciso accordo con le datazioni ottenute con le tecniche delle serie dell'uranio e definitivamente con l'eccellente accordo con i dati di paleomagnetismo e degli isotopi di ossigeno, la teoria è diventata la base per fornire la scala temporale di ogni tecnica che misuri il paleoclima.

Sono tre i parametri orbitali importanti (un quarto a cui accenneremo non è preso in considerazione da Milankovitch) che cambiano periodicamente: l'eccentricità, l'obliquità e l'inclinazione dell'asse terrestre (precessione degli equinozi)

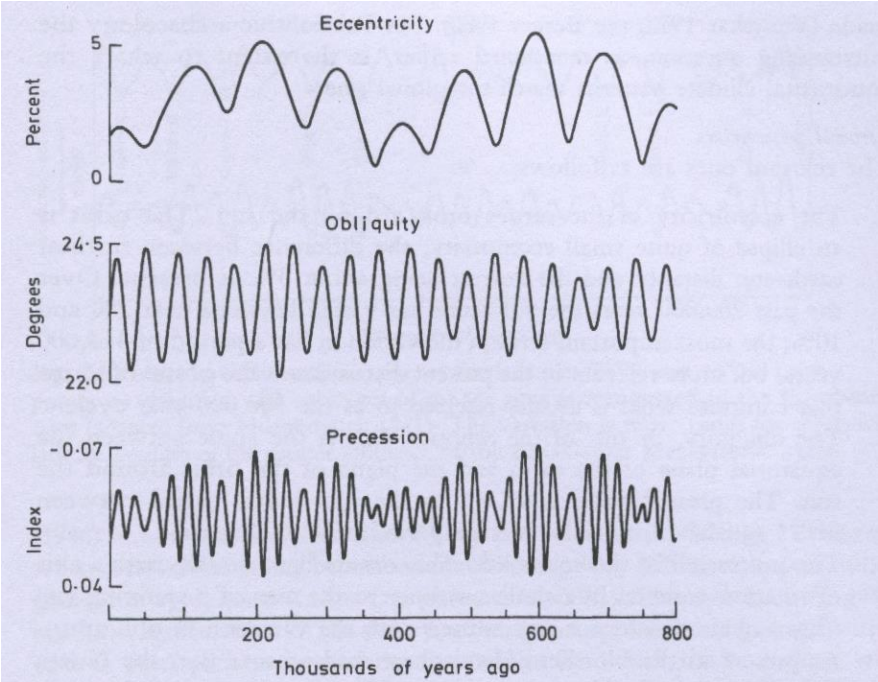

Fig. 2.6 Variation of orbital parameters (according to Berger 1977; redrawn from Imbrie and Imbrie 1980).

ECCENTRICITA'. L'orbita della terra intorno al sole non è circolare, ma ellittica. Attualmente c'è una differenza di circa il 3% tra distanza massima e minima dal sole, ma ora l'eccentricità è davvero piccola perché questa differenza oscilla tra un minimo del 2% ed un massimo del 10% (l'eccentricità varia quindi da un minimo dell' 1% ad un massimo del 5 %). C'è un periodo di circa 100.000 anni ed uno più lungo, di 413.000 anni.

$$e = \frac{d_a - d_p}{d_a + d_p} = 1 - \frac{2}{\frac{d_a}{d_p} + 1} = \frac{2}{\frac{d_p}{d_a} + 1} - 1$$

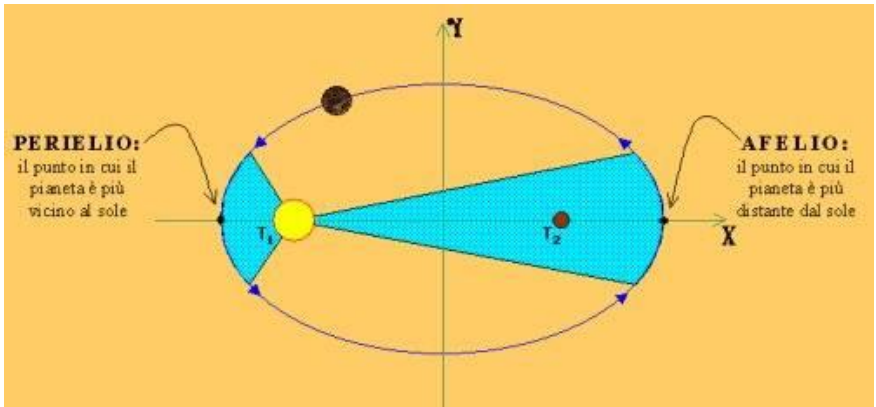

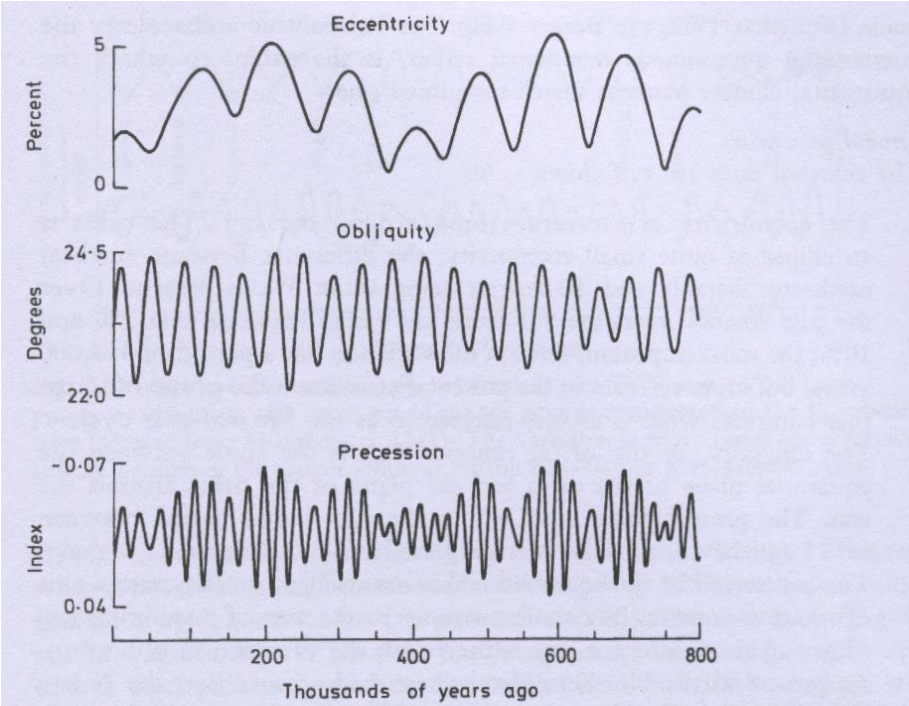

Fig. 2.6 Variation of orbital parameters (according to Berger 1977; redrawn from Imbrie and Imbrie 1980).

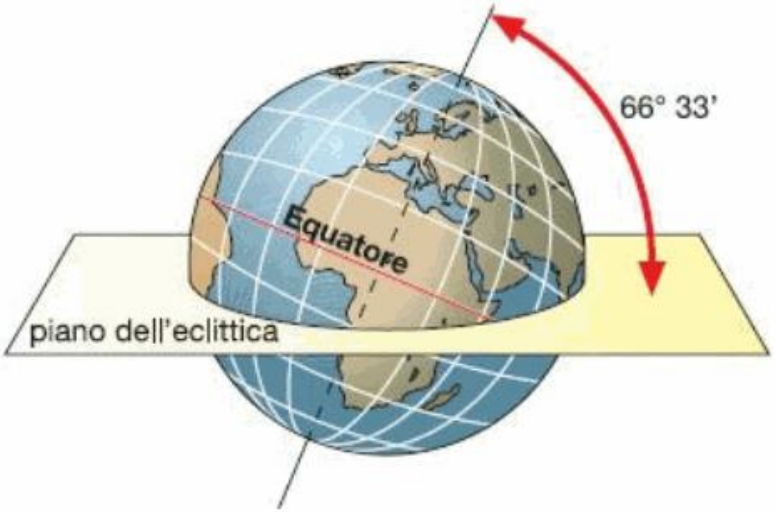

OBLIQUITA' (INCLINAZIONE). Angolo tra il piano equatoriale della terra ed il piano dell'orbita intorno al sole.

L'asse terrestre è inclinato rispetto alla perpendicolare al piano dell'eclittica: questa inclinazione, combinata con la rivoluzione della Terra intorno al Sole, è causa delle stagioni.

L'entità dell'inclinazione varia ciclicamente tra circa 22,5° e circa 24,5°, con un periodo di 41 000 anni; attualmente è di 23° 27′ e in diminuzione.

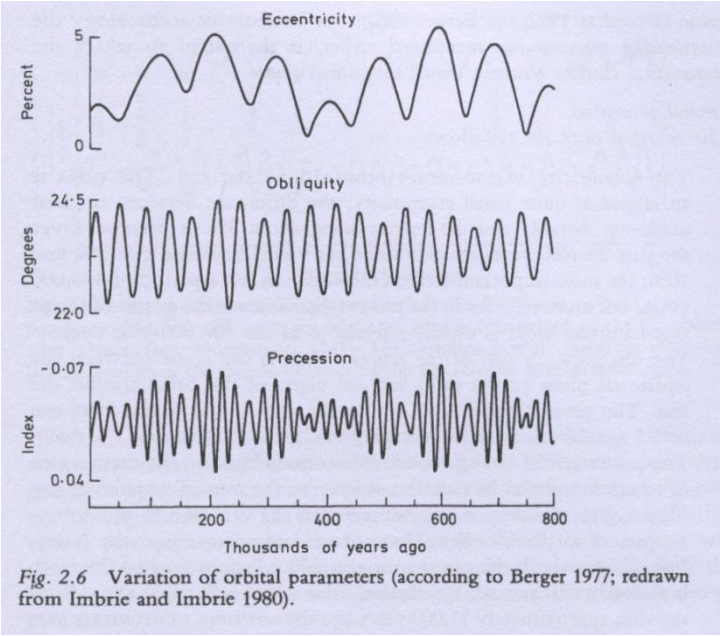

Fig. 2.6 Variation of orbital parameters (according to Berger 1977; redrawn from Imbrie and Imbrie 1980).

PRECESSIONE DEGLI EQUINOZI. L'asse di rotazione della terra, che ora punta nella direzione della stella polare, gira come quello di una trottola che precede. 10000 anni fa la stella polare era molto lontana dal polo nord.

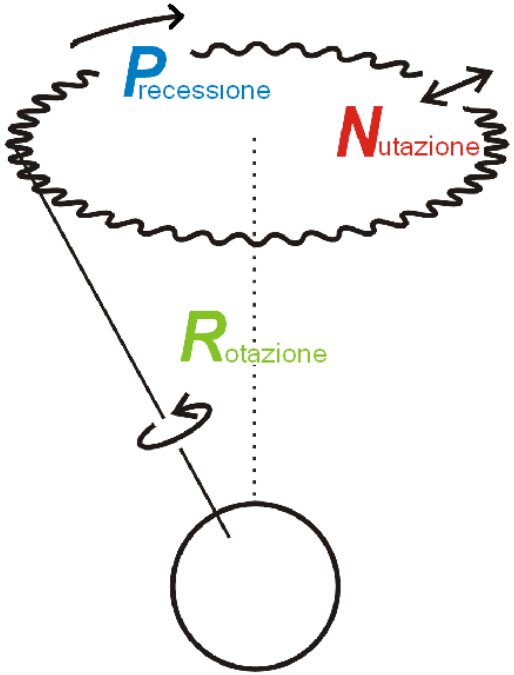

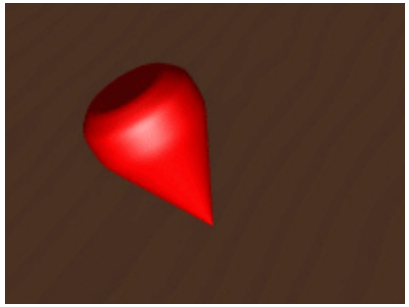

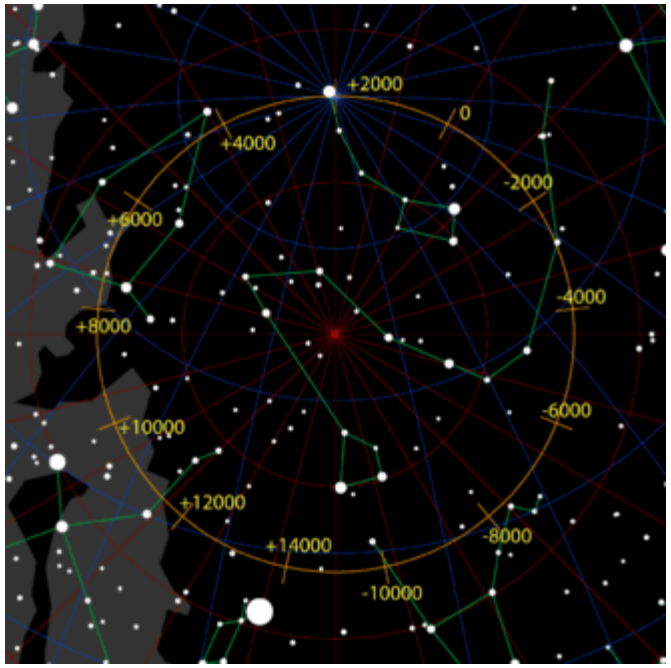

Cambiamento del polo nord celeste che si verifica nel corso di un anno platonico (25.800 anni) in seguito a un ciclo completo della precessione degli equinozi.

La precessione degli equinozi è dovuta alla forza di marea, esercitata dalla Luna e dal Sole.

Vi sono, infine, delle oscillazioni dell'asse di minore entità (circa 20″) e con un periodo più breve (circa 18,6 anni): quest'ultimo moto è detto nutazione.

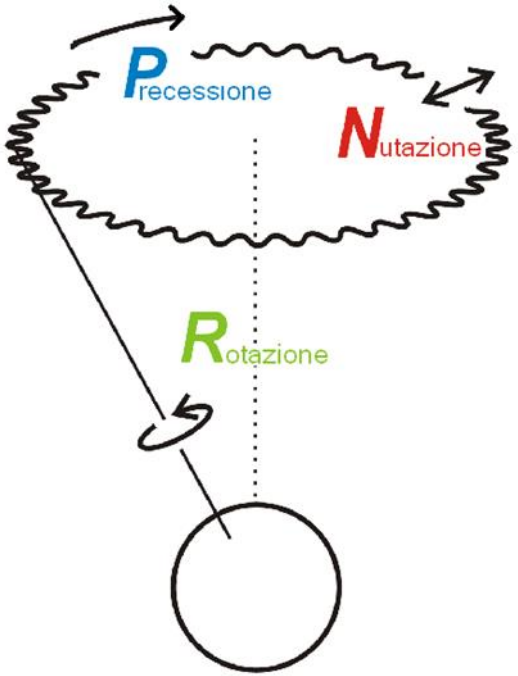

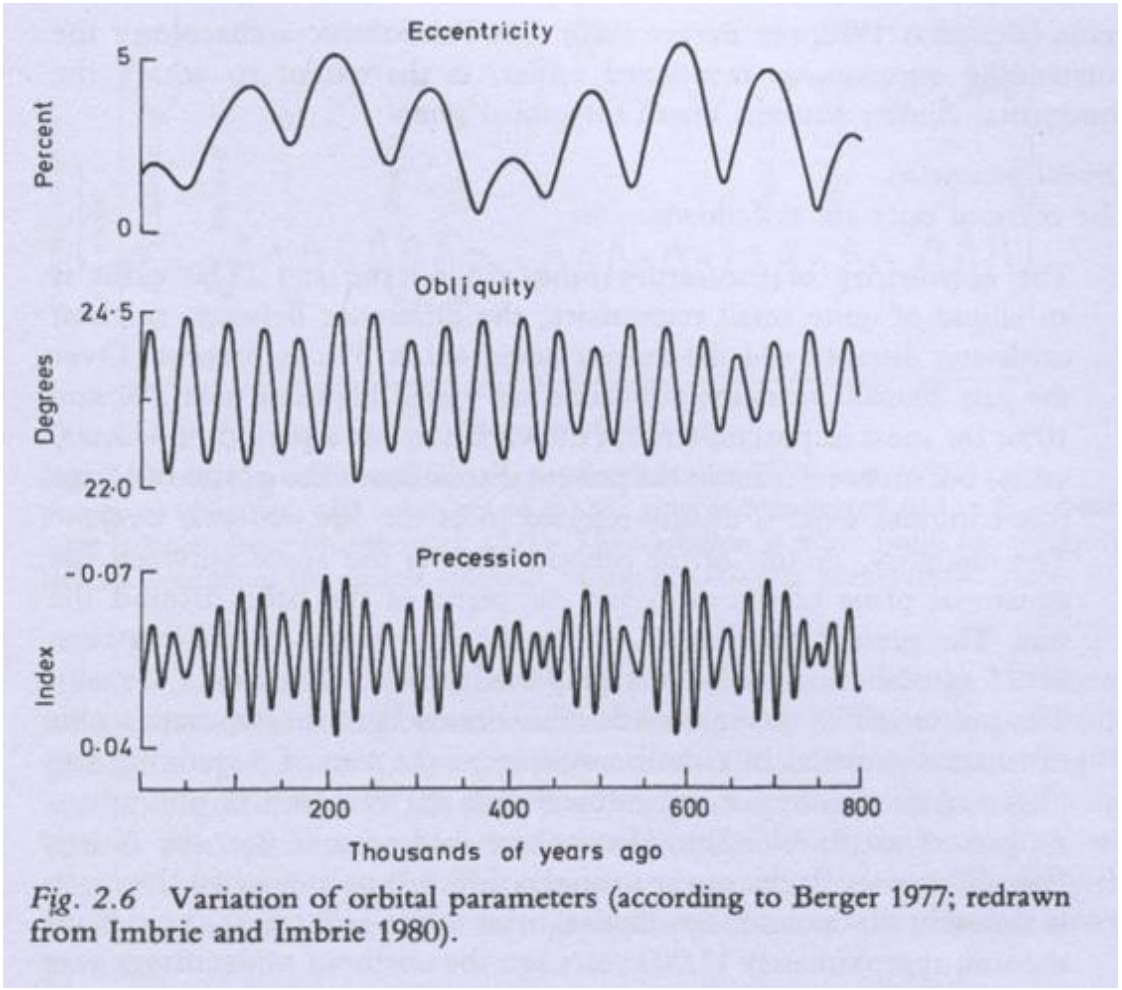

Fig. 2.6 Variation of orbital parameters (according to Berger 1977; redrawn from Imbrie and Imbrie 1980).

PERIODI

Due periodi
100.000 anni
e 410.000 anni

40.000 anni

25.800 anni

L’insolazione annuale totale non è influenzata dall’obliquità e dalla precessione e solo debolmente dalla eccentricità che ha causato fluttuazioni dell’ordine dell’ un per mille negli ultimi 500.000 anni. Il meccanismo è più sottile: il grado di contrasto tra le stagioni invernali ed estive. Quando il flusso di radiazione solare in estate nell’ emisfero settentrionale a grandi latitudini è più basso, allora si va verso un periodo glaciale con una risposta ritardata di qualche migliaia di anni (circa 8000 per l’obliquità).

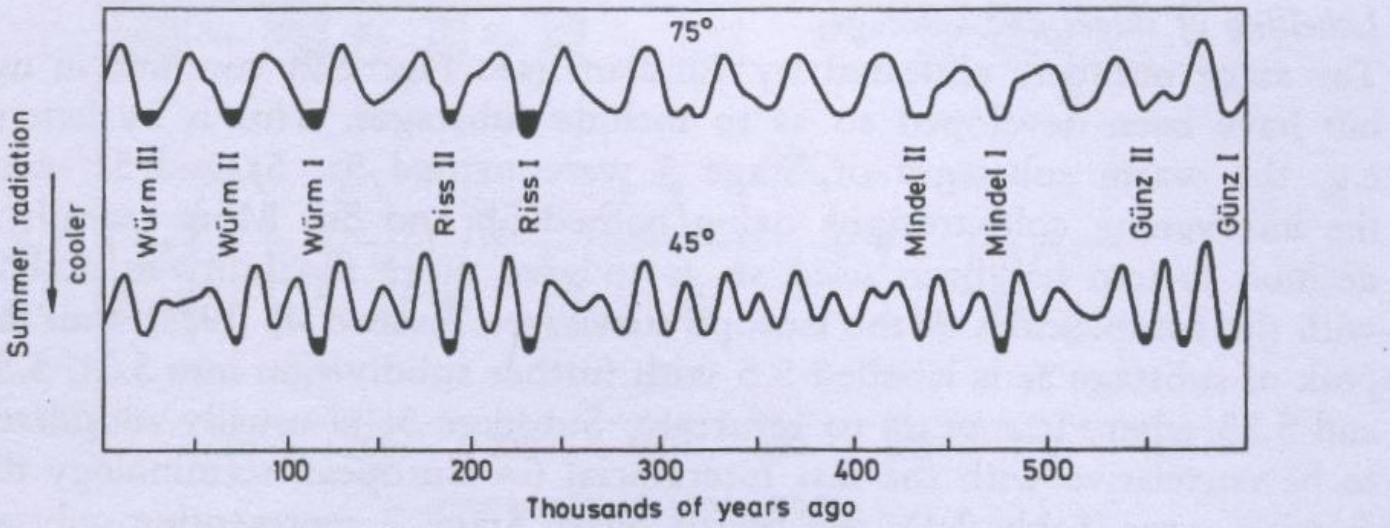

Fig. 2.5 Milankovitch insolation curves for latitudes 75°N and 45°N. Low points are identified with substages of the ice ages as recognized in the European Alps (adapted from Milankovitch 1941). The variation is more rapid for the lower latitude because of the greater influence of the 22,000-year precessional cycle.

Le oscillazioni calcolate in figura sono basate sui dati astronomici e riproducono, con peso diverso alle diverse latitudini, i periodi dei tre processi.

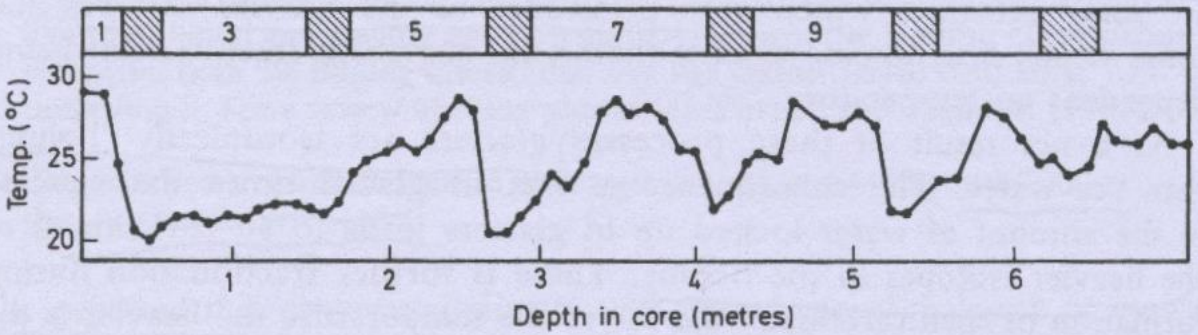

Fig. 2.2 Temperature variation for surface water of the Caribbean inferred by Emiliani (1955) from measurement of the oxygen–isotope ratio in planktonic foraminifera obtained from a core of sea-bottom sediment. Subsequently it was concluded that the major influence on the ratio was global ice-volume rather than water temperature. Hence the variation shown here is an overestimate. The stage numbers given at the top continue in use today; as will be seen warm stages have odd numbers and cold ones have even numbers (redrawn from Imbrie and Imbrie 1986).

In un primo tempo si era assegnato alla temperatura marina l'origine del frazionamento isotopico. Questo portava alla scala della figura sopra per le variazioni di temperatura. Poi si è scoperto che l'effetto principale era invece il frazionamento isotopico nella formazione dei ghiacci per cui una scala più corretta ricostruisce cambi di temperatura molto minori (circa un terzo di quelli riportati in figura).

Riassumendo, prima si sono usati i metodi del C14, delle serie dell'uranio e dell'inversione magnetica per la datazione della stratigrafia. Poi, una volta convinti che queste datazioni erano in accordo con le previsioni astronomiche, una scala astronomica dei tempi è stata presa come base dell'analisi dei dati e la costruzione della storia del paleoclima.

Questo ha inoltre permesso di rendere più precise le altre tecniche.

Ha anche permesso di fare previsioni per il futuro che prevederebbe presto una nuova fase glaciale, anche se al momento ci stiamo dando un pò troppo da fare per contrastarla!

Vedremo poi che le più recenti prospezioni del ghiaccio antartico hanno permesso datazioni molto precise per gli ultimi 800.000 anni. Queste hanno fatto rivederele precedenti scale temporali relative a tutte le altre prospezioni sia marine che terrestri che glaciali in Groenlandia.

Table 2.4 Oxygen-isotopic stage boundaries

Boundary [a]	*Termination* [b]	*Ages (thousands of years)*		
		Shackleton[c] *and Opdyke (1973, 1976)*	*Imbrie*[d] *et al. (1984)*	*Martinson*[d] *et al. (1987)*
1–2	I	13	12	12
2–3		32	24	24
3–4		64	59	60
4–5		75	71	74
5–6	II	128	128	130
6–7		195	186	190
7–8	III	251	245	244
8–9		297	303	
9–10	IV	347	339	
10–11		367	362	
11–12	V	440	423	
12–13		472	478	
13–14		502	524	
14–15		542	565	
15–16	VI	592	620	
16–17		627	659	
17–18		647	689	
18–19		688	726	
19–20			736	
20–21			763	
21-22			790	

[a] In the terminology of Pisias *et al.* (1984) successive boundaries, reading from the top, are denoted by 2.0, 3.0, 4.0, etc.

[b] The terminations are those defined by Broecker and van Donk (1970) on the basis of their interpretation of the saw-toothed character of their record.

[c] The ages in this core are based on 700,000 years for the Brunhes–Matuyama boundary and the assumption of a constant sedimentation rate. The revised age for that boundary is 730,000 ± 11,000 years (Mankinen and Dalrymple 1979).

[d] The ages are astronomically based with an estimated overall accuracy of 5000 years.

Questa tabella (un po' datata) confronta le date proposte da diverse scuole per il passaggio da una fase glaciale ad una interglaciale

CAROTAGGIO NEI GHIACCIAI

Registri del rapporto isotopico dell'ossigeno si trovano anche nei ghiacciai, in ottimo accordo con quelli dei carotaggi dei sedimenti oceanici. In una carota lunga 2 km prelevata in Groenlandia è stato possibile rivelare gli strati annuali di più di 5000 anni, spessi più di 10 cm vicino alla superficie e che si assottigliano mano a mano che si va più a fondo. Notare che qui si vedono gli strati anno per anno. Nelle carote antartiche, invece, si arriva a circa un milione di anni e la precisione di datazione è di qualche migliaio di anni. Oltre agli isotopi dell'ossigeno, per il ghiaccio è interessante anche la concentrazione del deuterio. Inoltre si misura l'acidità e la concentrazione delle polveri.

In particolare è stato possibile rivelare gli effetti di alcune eruzioni vulcaniche della storia recente e in base a queste esperienze datare l'eruzione di Thera (Santorini nel mare Egeo). Un eruzione immette nell'atmosfera grandi quantità di polveri e di solfuri. Gli aerosol di acido solforico raggiungono la stratosfera e vi soggiornano per mesi. La neve cade acida e questa acidità viene rilevata in uno strato della carota di ghiaccio. Gli effetti delle più importanti eruzioni, che diminuiscono l'insolazione per l'oscuramento da polveri attenuando il ritmo di crescita delle piante, sono rivelati anche dalla dendrocronologia.

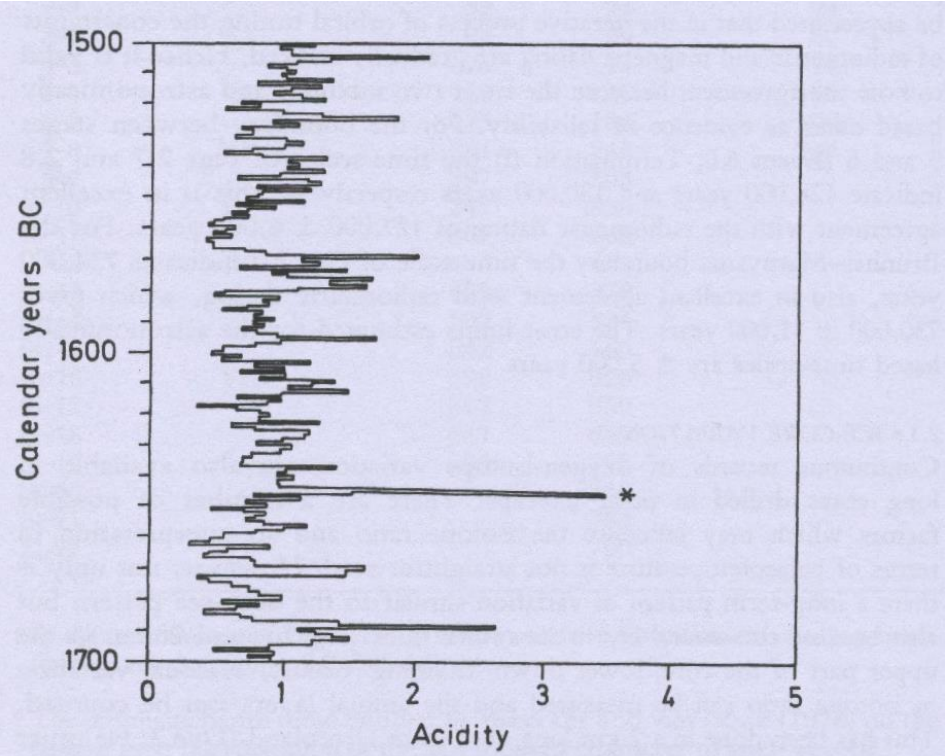

Fig. 2.9 Part of the acidity record from the Dye–3 core, Greenland (redrawn from Hammer *et al.* 1987). Of the two prominent peaks in these two centuries only the one marked with a star is considered to be due to a volcanic eruption. This is because the acidity in the ice layer concerned was predominantly due to sulphuric acid (see Fig. 2.10), whereas the other peak was dominated by nitric acid (indicative of intense melting during summer months). The acidity is measured by means of a special electric conductometric method having a resolution of a few millimetres; it is expressed in terms of equivalent hydrogen-ion concentration.

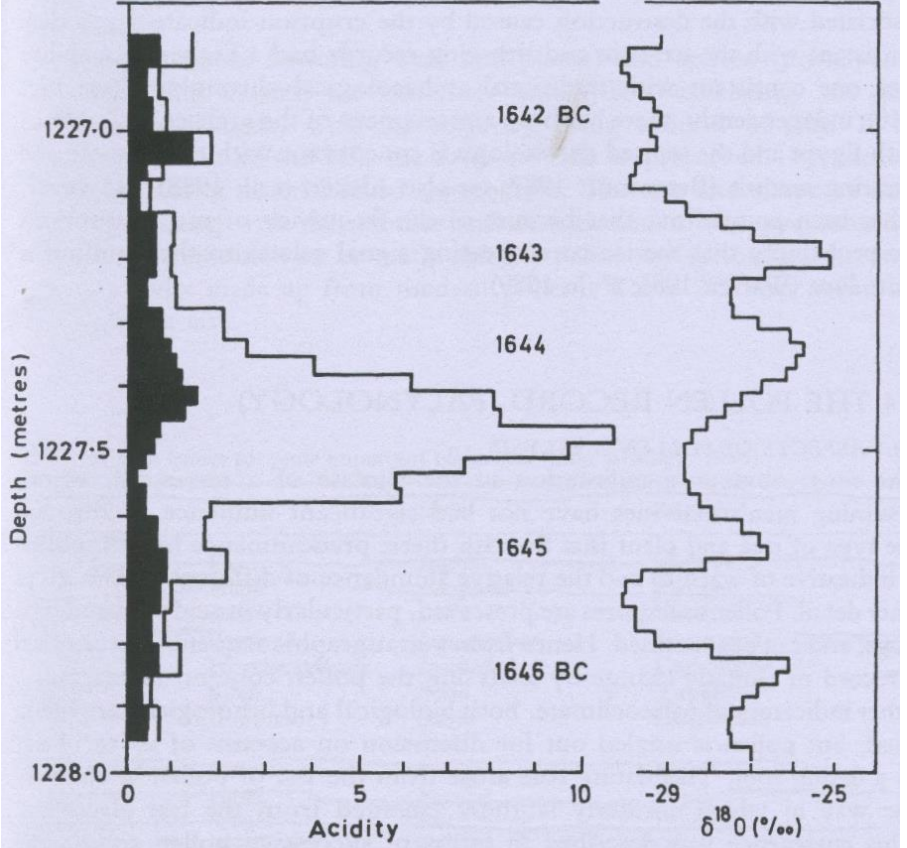

Fig. 2.10 More detail (redrawn from Hammer *et al.* 1987) relevant to the starred peak of Fig. 2.9. The filled histogram on the left of the figure represents nitric acid concentration and the unfilled histogram sulphuric acid plus nitric acid; these concentrations were determined by chemical analysis (ion chromatography). Oxygen–isotope values are shown on the right with calendar dates being given in the middle. The rightward peaks (less negative $\delta^{18}O$) correspond to summer.

Il carotaggio in Groenlandia segnala un evento con alto picco di acidità datato al 1644±20 BC.

La dendrocronologia data l'evento al 1628±20 BC, concorde entro l'errore.

La cronologia archeologica, basata sui ritrovamenti e ancorata al calendario egiziano data l'evento un secolo dopo. Ma la cronologia del C14 sembra dar ragione alle prime due e suggerisce di rivedere la cronologia archeologica.

NATURE VOL. 329 1 OCTOBER 1987

Vostok ice core provides 160,000-year record of atmospheric CO_2

J. M. Barnola*, D. Raynaud*, Y. S. Korotkevich† & C. Lorius*

* Laboratoire de Glaciologie et de Géophysique de l'Environnement, BP 96, 38402 Saint Martin d'Hères Cedex, France
† Arctic and Antarctic Research Institute, Beringa Street 38, Leningrad 199226, USSR

Direct evidence of past atmospheric CO_2 changes has been extended to the past 160,000 years from the Vostok ice core. These changes are most notably an inherent phenomenon of change between glacial and interglacial periods. Besides this major 100,000-year cycle, the CO_2 record seems to exhibit a cyclic change with a period of some 21,000 years.

ALTHOUGH the first direct CO_2 measurements in the atmosphere were made in the second half of the nineteenth century, atmospheric CO_2 variations have been monitored in a systematic and reliable manner only since 1958. Fortunately, nature has been taking continuous samples of the atmosphere at the surface of the ice sheets throughout the ages. This natural sampling process takes place when snow is transformed into ice by sintering at the surface of the melt-free zones of the ice sheets, with air becoming isolated from the surrounding atmosphere in the pores of the newly formed ice. After pore closure the gas remains stored in the ice moving within the ice sheet. During this natural air sampling and storage process, different mechanisms could alter the original atmospheric composition[1,2]. But by choosing appropriate sampling sites, ice cores (for example see ref. 1) and experimental methods[3], past CO_2 changes in the atmosphere can be determined with high confidence by analysing the air enclosed in the pores of the ice.

Because of the extremely low temperatures at Vostok (present-day mean annual temperature is −55.5 °C) and the good core quality, the 2,083-m-long ice core recovered by the Soviet Antarctic Expeditions at Vostok (East Antarctica) provides a unique opportunity to extend the ice record of atmospheric CO_2 over the last glacial–interglacial cycle back to the penultimate ice age about 160 kyr ago[11]. Over this timescale a high correlation is found between CO_2 concentrations and Antarctic climate, with significant oscillatory behaviour of CO_2 between high levels during interglacial and low levels during glacial periods. The CO_2 record also seems to exhibit a cyclic change with a period of ~21 kyr, that is, around the orbital period corresponding to the precession.

Experimental procedure

Gas extraction and measurements were performed with the 'Grenoble analytical setup' described by Barnola *et al.*[12]. The method is based on crushing the ice under vacuum without melting, expanding the gas released during the crushing in a pre-evacuated sampling loop, and analysing the CO_2 concentrations by gas chromatography.

The analytical system, except for the stainless steel container in which the ice is crushed, is calibrated for each ice sample measurement with a standard mixture of CO_2 in nitrogen and oxygen. The corresponding accuracy (2σ) is evaluated from the standard deviation of the residuals corresponding to the calibration regression and ranges from 3 to 12 parts per million by volume (p.p.m.v.) for the measurements presented in this article.

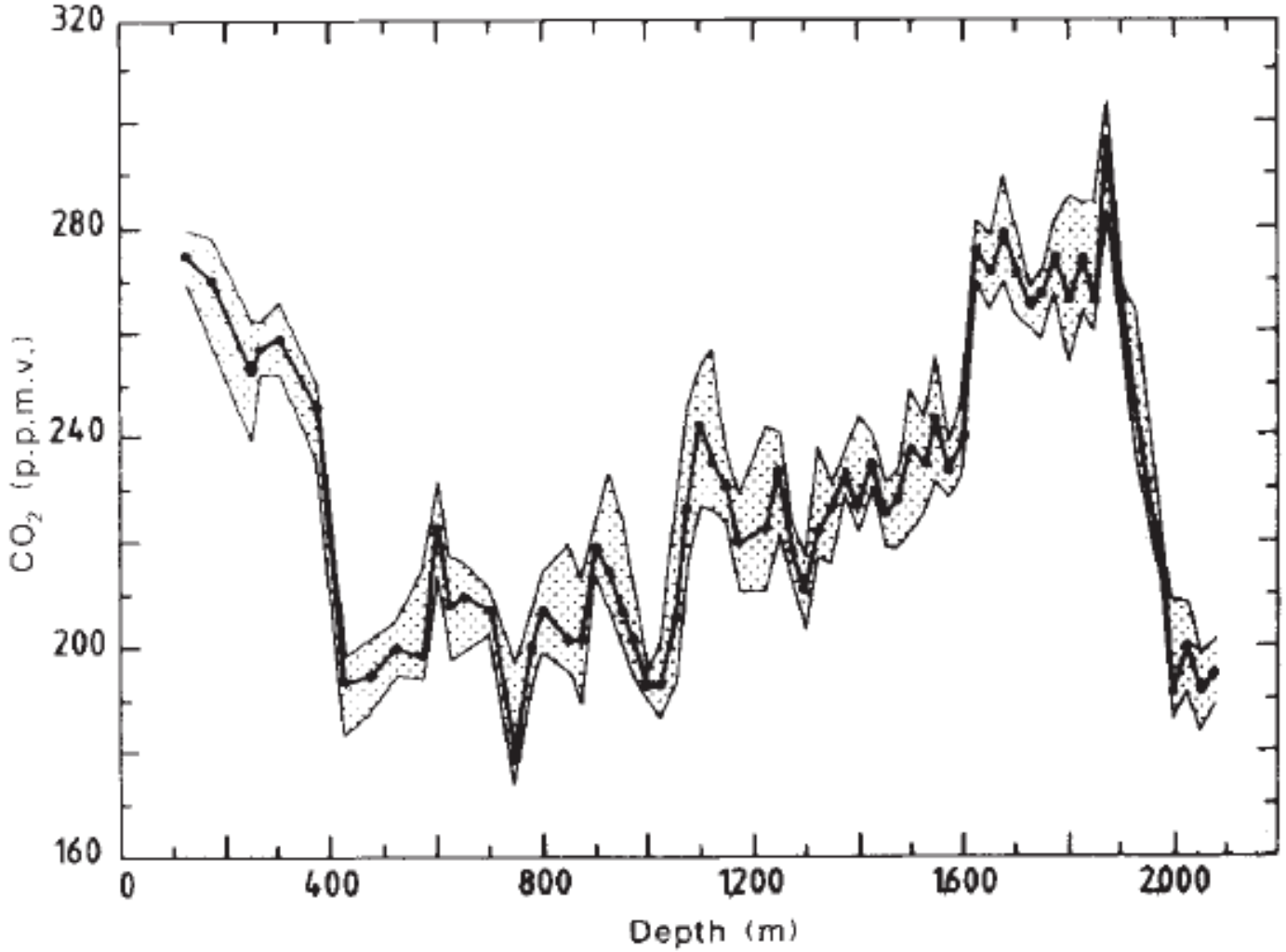

Fig. 1 CO_2 concentrations (p.p.m.v.) plotted against depth in the Vostok ice core. The 'best estimates' of the CO_2 concentrations are indicated by dots and the envelope shown has been plotted taking into account the different uncertainty sources.

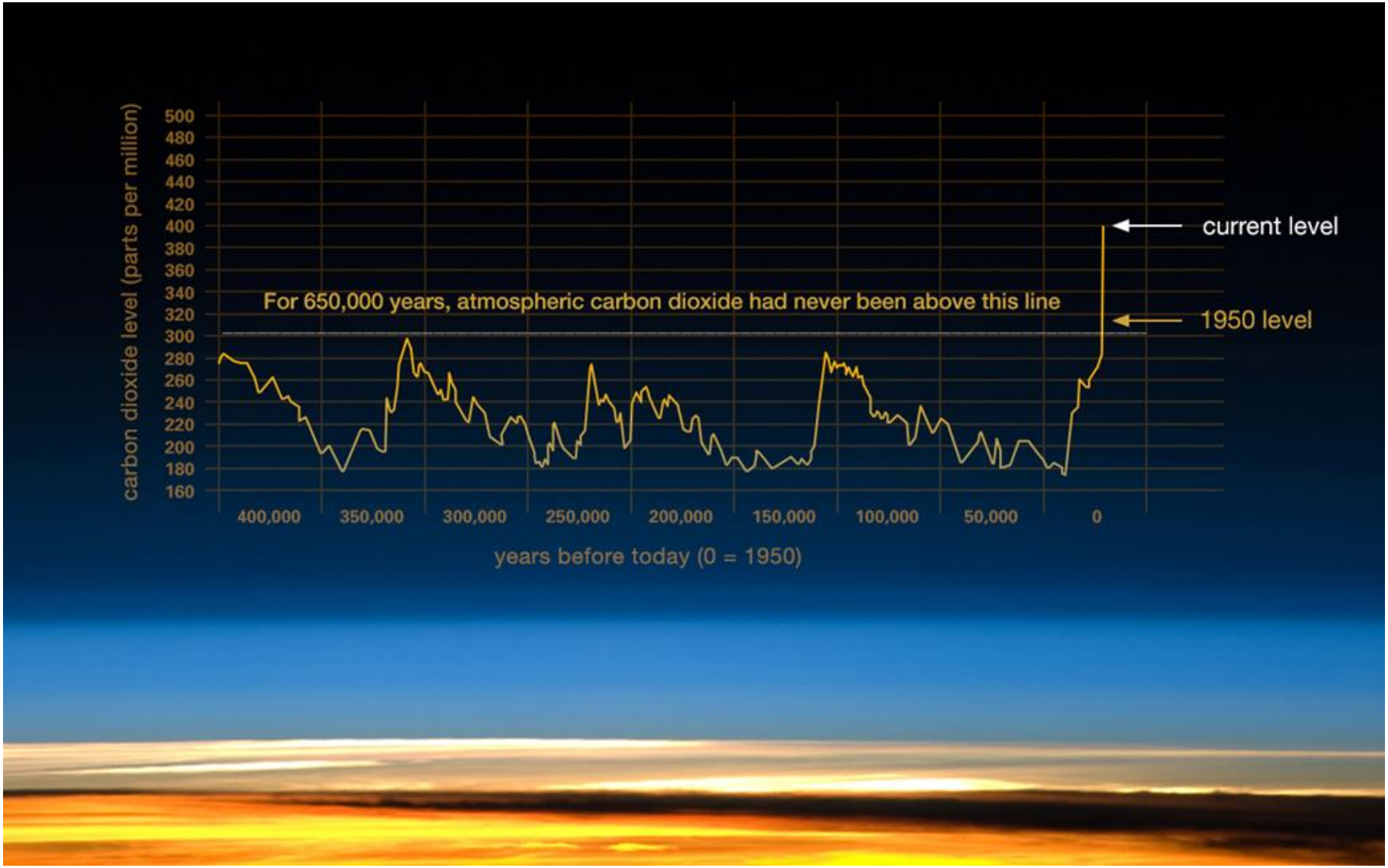

NASA This graph, based on the comparison of atmospheric samples contained in ice cores and more recent direct measurements, provides evidence that atmospheric CO_2 has increased since the Industrial Revolution. (Credit: Vostok ice core data/J.R. Petit et al.; NOAA Mauna Loa CO2 record.)

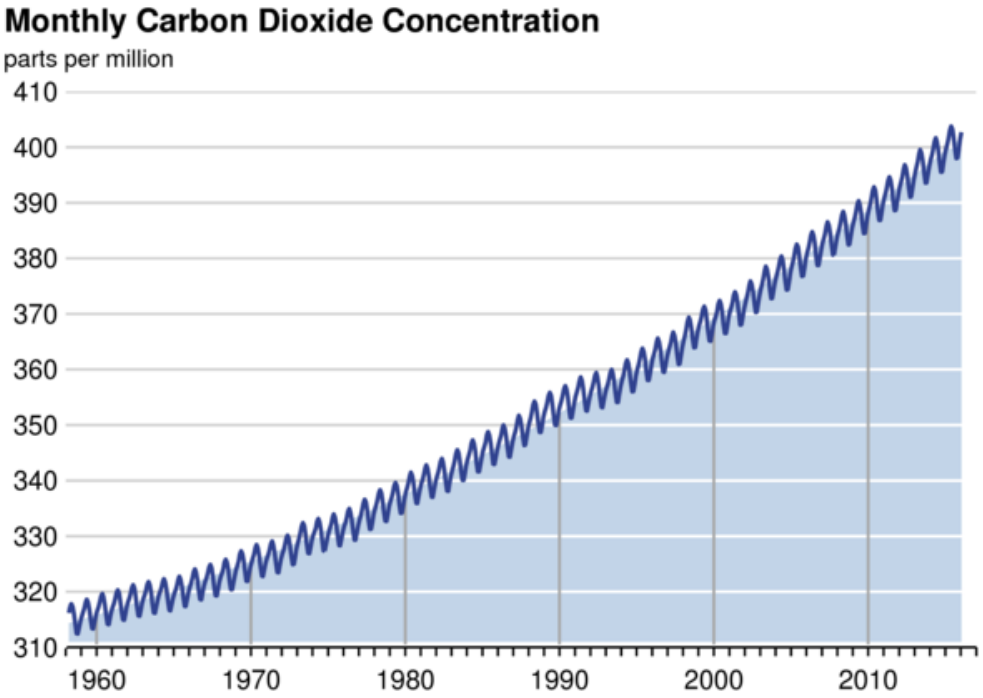

http://scrippsco2.ucsd.edu/

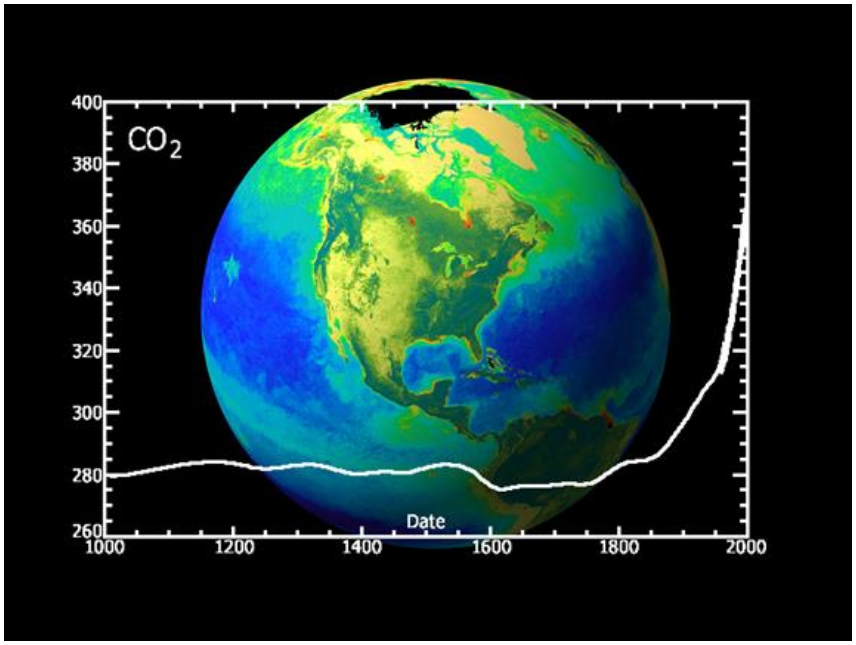

Mauna Loa Observatory, Hawaii

The following assumptions have been made to date the air in relation to the ice: (1) the air in the firn layers is well mixed with the atmosphere until firn pores close; (2) pore closure occurs roughly in the firn density interval 0.80–0.83 (ref. 13), that is, in the deepest layers of the firn (found between about 86 and 96 m depth at Vostok); and (3) the density–depth profile has remained unchanged over the past 160 kyr.

Based on these assumptions the difference between the age of the ice and the mean age of the air, which is dependent on accumulation rate, is evaluated taking into account the temporal changes of the accumulation rate[11]. This calculated difference varies between about 2,500 yr for the warmest to about 4,300 yr for the coldest periods.

On the other hand, all the air enclosed in an ice sample has not been pinched off from the atmosphere at the same time but rather pore after pore over a time interval which, with the above assumptions, lies between 300 and 750 yr. This acts as a low-pass filter and means that each CO_2 measurement represents roughly an average value over several hundred years.

Microstructure, specifically open pore structure, and not density, is the main parameter controlling the permeability and gas transport in polar firn. Pore structure is the direct result of microstructure resulting from the initial depositional processes and post-depositional metamorphism controlled by accumulation rate when the firn was near the surface of the ice sheet. Pore close-off will occur when the pore structure restricts air movement, causing the firn layer to become impermeable independent of the density of the layer.

Description. Sixty-six depth levels were investigated for CO_2 measurements along the 2,083-m core. They are spaced every ~25 m from 850 m depth to the bottom. Because of the presence of fractures in the upper part of the core, the spacing is generally larger above 850 m depth. With this sampling, the mean age difference between two neighbouring levels ranges from ~2,000 to ~4,500 yr.

The record covers the past ~160 kyr and includes the following major climatic periods: the Holocene, the last glaciation, the previous interglacial and the end of the penultimate glaciation[11,14]. Figure 1 shows the results (best estimates and envelope obtained as described above) plotted against depth. Figure 2 shows the CO_2 variations with age of the air.

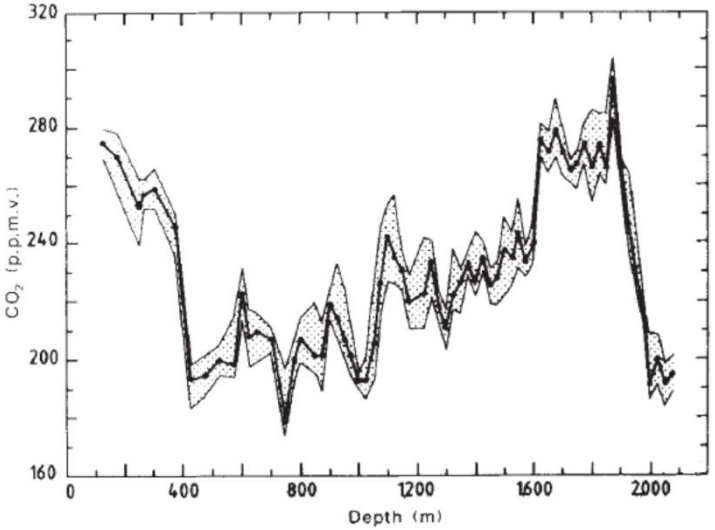

Fig. 1 CO_2 concentrations (p.p.m.v.) plotted against depth in the Vostok ice core. The 'best estimates' of the CO_2 concentrations are indicated by dots and the envelope shown has been plotted taking into account the different uncertainty sources.

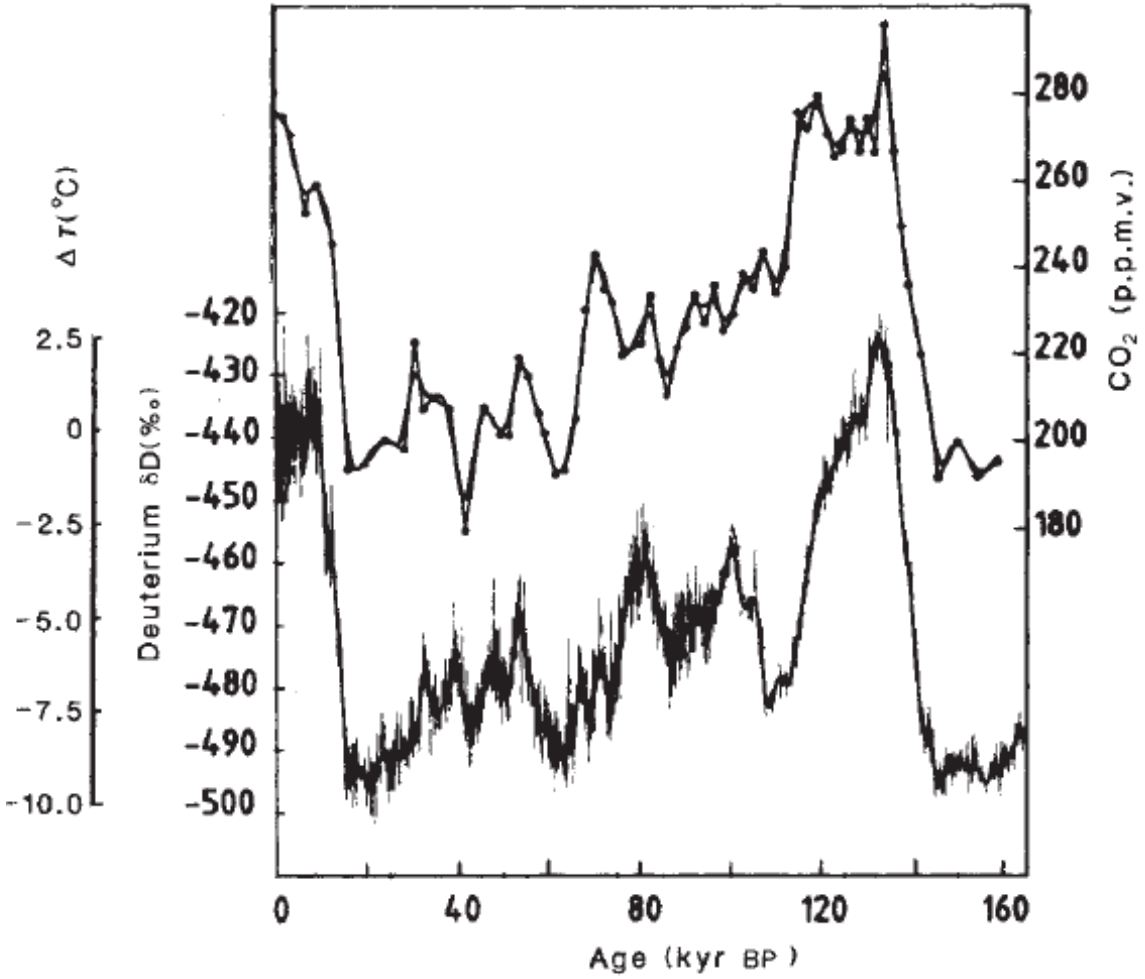

Fig. 2 CO_2 concentrations ('best estimates') and smoothed values (spline function) in p.p.m.v. plotted against age in the Vostok record (upper curves) and atmospheric temperature change derived[14] from the isotopic profile (lower curve). The deuterium scale corresponds to values after correction for deuterium changes of oceanic water[14].

The CO_2 record exhibits two very large changes, one near the most recent part of the record (~400 m depth or 15 kyr BP) and the other near the earliest part of the record (~1,950 m depth or 140 kyr BP), between two levels centred on 190–200 and 260–280 p.p.m.v. roughly typical of the lowest and highest values of the whole record. The high level is comparable with the so-called 'pre-industrial' CO_2 level that prevailed roughly 200 years ago, just before the large anthropogenic disturbance of the CO_2 cycle; the low level ranges among the lowest values of the known geological history of carbon dioxide over the last 10^8 yr (ref. 15). These two large CO_2 changes correspond to the transitions between full glacial conditions (low CO_2) of the last and penultimate glaciations, and the two major warm periods (high CO_2) of the record: the Holocene and the previous interglacial.

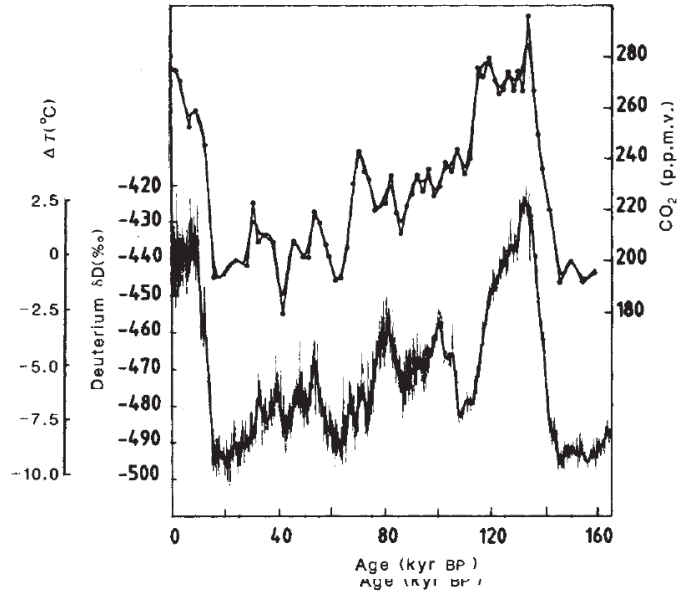

Between these two extremities of the record, that is, over the period covering mainly the last glaciation, the CO_2 shows a general decreasing trend with the lowest values found over the last part of the glaciation (between ~1.025 and 425 m depth, or 65 and 15 kyr) and with two marked breaks: a first decrease of ~40 p.p.m.v. at ~1,610 m depth (~114 kyr BP), and a second of ~50 p.p.m.v. at ~1,070 m depth (~68 kyr BP). Other CO_2 changes are superimposed on the general decreasing trend, suggesting an oscillatory behaviour with an apparent period of ~20 kyr, especially between ~80 and 20 kyr BP. These changes are more pronounced in the last part of the glaciation, but note that some of the variability observed above 850 m depth could be due to the lower ice quality in that part of the core.

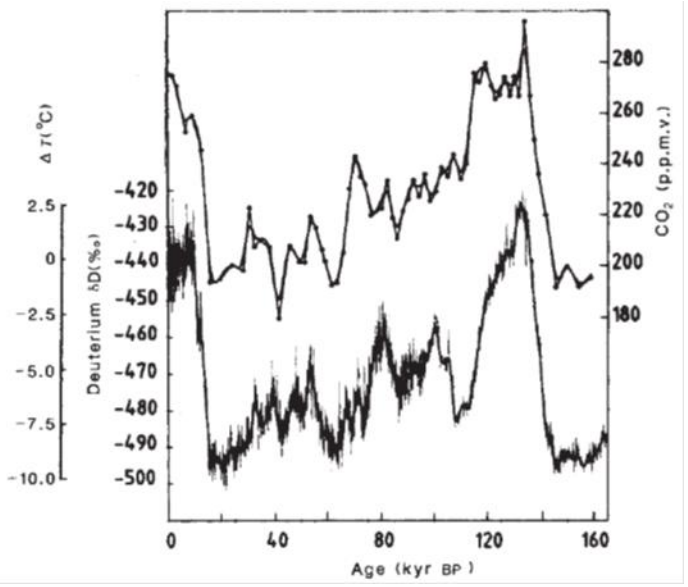

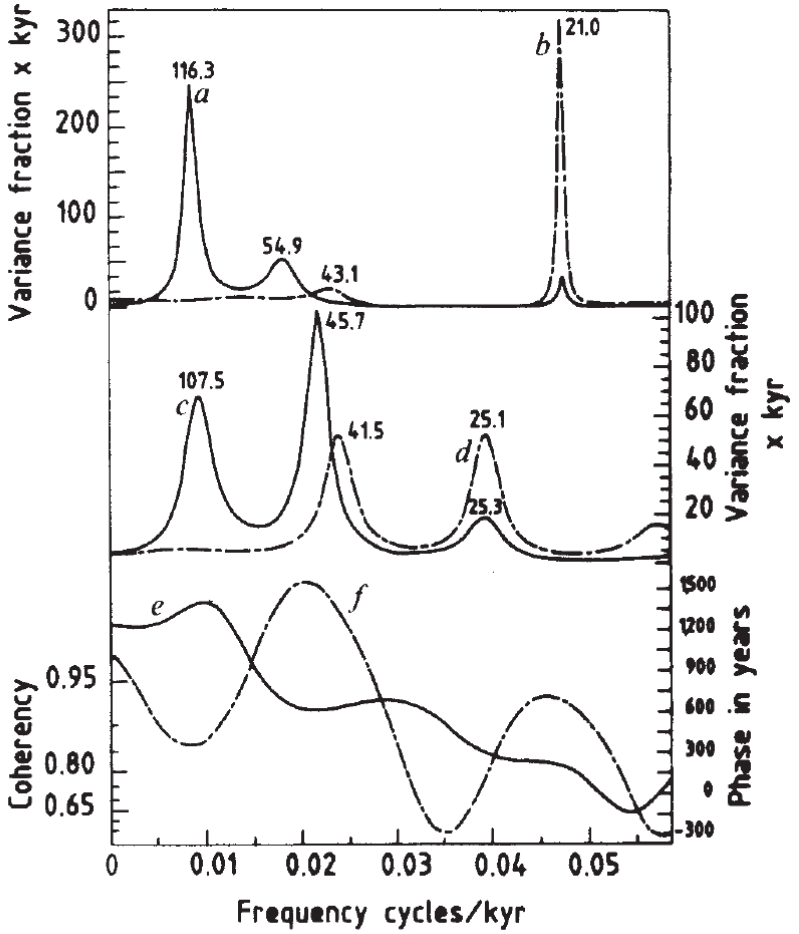

Fig. 3 *a*, *b*, Variance spectra of the Vostok CO_2 record. The normalized variance density is plotted against frequency in cycles per kyr. The continuous line (*a*) refers to the original series and the dashed line (*b*) to the series after prewhitening by a first-order difference filter. The spectra were obtained by the ME method applying the Barrodale and Ericksson algorithm with an autoregressive order of 40%. *c*, *d*, Variance spectra of the Vostok isotope temperature record from ref. 14, obtained with the same procedure. *e*, *f*, Cross-spectral analysis between CO_2 and temperature for coherency (*e*) and phase spectrum (*f*), obtained by applying the Blackman–Tukey method. The phase (right scale) is positive when CO_2 lags the temperature.

Andamento ciclico?
Periodicità da confrontare con astronomical cycling forcing of climate?

Analisi spettrale!
Trasformata di Fourier.
Ma il periodo studiato (160 ky) è corto rispetto ai periodi astronomici (da circa 20 ky a più di 100 ky).

Un decisivo passo in avanti è stato fatto quando si è capito che la misura del rapporto tra ossigeno e azoto era in grado di fornire una datazione precisa della stratigrafia delle carote antartiche.

Nature **448**, 912-916 (23 August 2007) | doi:10.1038/nature06015; Received 14 April 2007; Accepted 12 June 2007

Northern Hemisphere forcing of climatic cycles in Antarctica over the past 360,000 years

Kenji Kawamura[1,2,9], Frédéric Parrenin[3], Lorraine Lisiecki[4], Ryu Uemura[5], Françoise Vimeux[6,7], Jeffrey P. Severinghaus[2], Manuel A. Hutterli[8], Takakiyo Nakazawa[1], Shuji Aoki[1], Jean Jouzel[7], Maureen E. Raymo[4], Koji Matsumoto[1,9], Hisakazu Nakata[1,9], Hideaki Motoyama[5], Shuji Fujita[5], Kumiko Goto-Azuma[5], Yoshiyuki Fujii[5] & Okitsugu Watanabe[5]

Center for Atmospheric and Oceanic Studies, Graduate School of Science, Tohoku University, Sendai 980-8578, Japan

Scripps Institution of Oceanography, University of California, San Diego, 9500 Gilman Drive, La Jolla, California 92093-0244, USA

Laboratoire de Glaciologie et Geophysique de l'Environnement, CNRS/UJF, 54 rue Molière, 38400 Grenoble, France

Department of Earth Sciences, Boston University, 685 Commonwealth Avenue, Boston, Massachusetts 02215, USA

National Institute of Polar Research, Research Organization of Information and Systems, 1-9-10 Kaga, Itabashi-ku, Tokyo 173-8515, Japan

Institut de Recherche pour le Développement (IRD), UR Great Ice

IPSL/LSCE, Laboratoire des Sciences du Climat et de l'Environnement, UMR CEA-CNRS-UVSQ, CE Saclay, Orme des Merisiers, 91191 Gif-sur-Yvette, France

British Antarctic Survey, High Cross, Madingley Road, Cambridge CB3 0ET, UK

Present addresses: National Institute of Polar Research, Research Organization of Information and Systems, 1-9-10 Kaga, Itabashi-ku, Tokyo 173-8515, Japan (K.K.); Japan Meteorological Agency, 1-3-4 Otemachi, Chiyoda-ku, Tokyo 100-8122, Japan (K.M.); Japan Atomic Energy Agency, Tokai-mura, Ibaraki 319-1195, Japan (H.N.).

The Milankovitch theory of climate change proposes that glacial–interglacial cycles are driven by changes in summer insolation at high northern latitudes[1]. The timing of climate change in the Southern Hemisphere at glacial–interglacial transitions (which are known as terminations) relative to variations in summer insolation in the Northern Hemisphere is an important test of this hypothesis. So far, it has only been possible to apply this test to the most recent termination[2, 3], because the dating uncertainty associated with older terminations is too large to allow phase relationships to be determined. Here we present a new chronology of Antarctic climate change over the past 360,000 years that is based on the ratio of oxygen to nitrogen molecules in air trapped in the Dome Fuji and Vostok ice cores[4, 5]. This ratio is a proxy for local summer insolation[5], and thus allows the chronology to be constructed by orbital tuning without the need to assume a lag between a climate record and an orbital parameter. The accuracy of the chronology allows us to examine the phase relationships between climate records from the ice cores[6, 7, 8, 9] and changes in insolation. Our results indicate that orbital-scale Antarctic climate change lags Northern Hemisphere insolation by a few millennia, and that the increases in Antarctic temperature and atmospheric carbon dioxide concentration during the last four terminations occurred within the rising phase of Northern Hemisphere summer insolation. These results support the Milankovitch theory that Northern Hemisphere summer insolation triggered the last four deglaciations.

Because O_2 molecules are preferentially excluded from freshly formed air bubbles during the snow–ice transition, the O_2/N_2 ratio of air trapped in Antarctic ice is depleted by 5–10 on average from the atmospheric ratio. The O_2/N_2 in the Vostok[5] and Dome Fuji[4] cores (Fig. 1) varies in accordance with local summer insolation with an amplitude of 10 , with stronger insolation leading to more O_2/N_2 depletion. Local summer insolation presumably controls the physical properties of near-surface snow, which in turn determines the magnitude of O_2/N_2 fractionation during the bubble close-off[5]. The O_2/N_2 records of Antarctic inland cores are expected to be in phase with summer solstice insolation. Support for this view comes from the present-day observation at Dome Fuji of maxima within several days of the solstice in snow temperature (10-cm depth) and vertical temperature gradient (between 10 and 50 cm) both of which are important factors for snow metamorphism[5]. Positive feedback between snow grain size and absorption of solar radiation, as well as a negative relationship between surface albedo and solar zenith angle, increases the importance of the solstice[5].

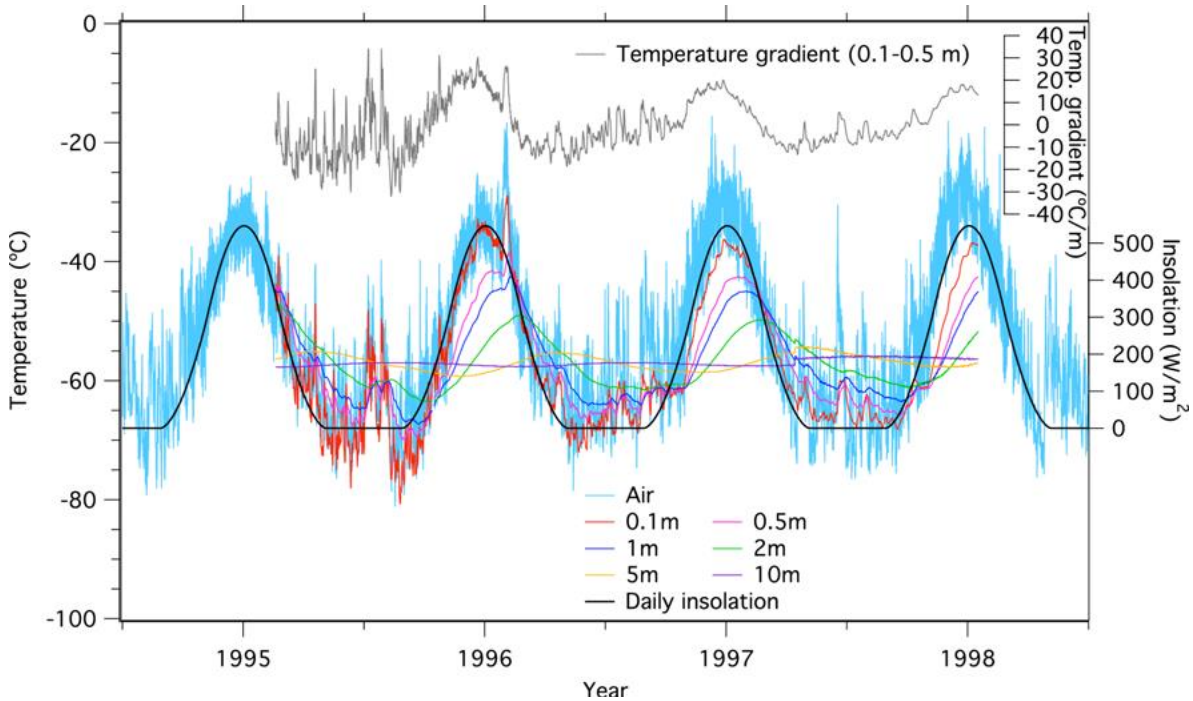

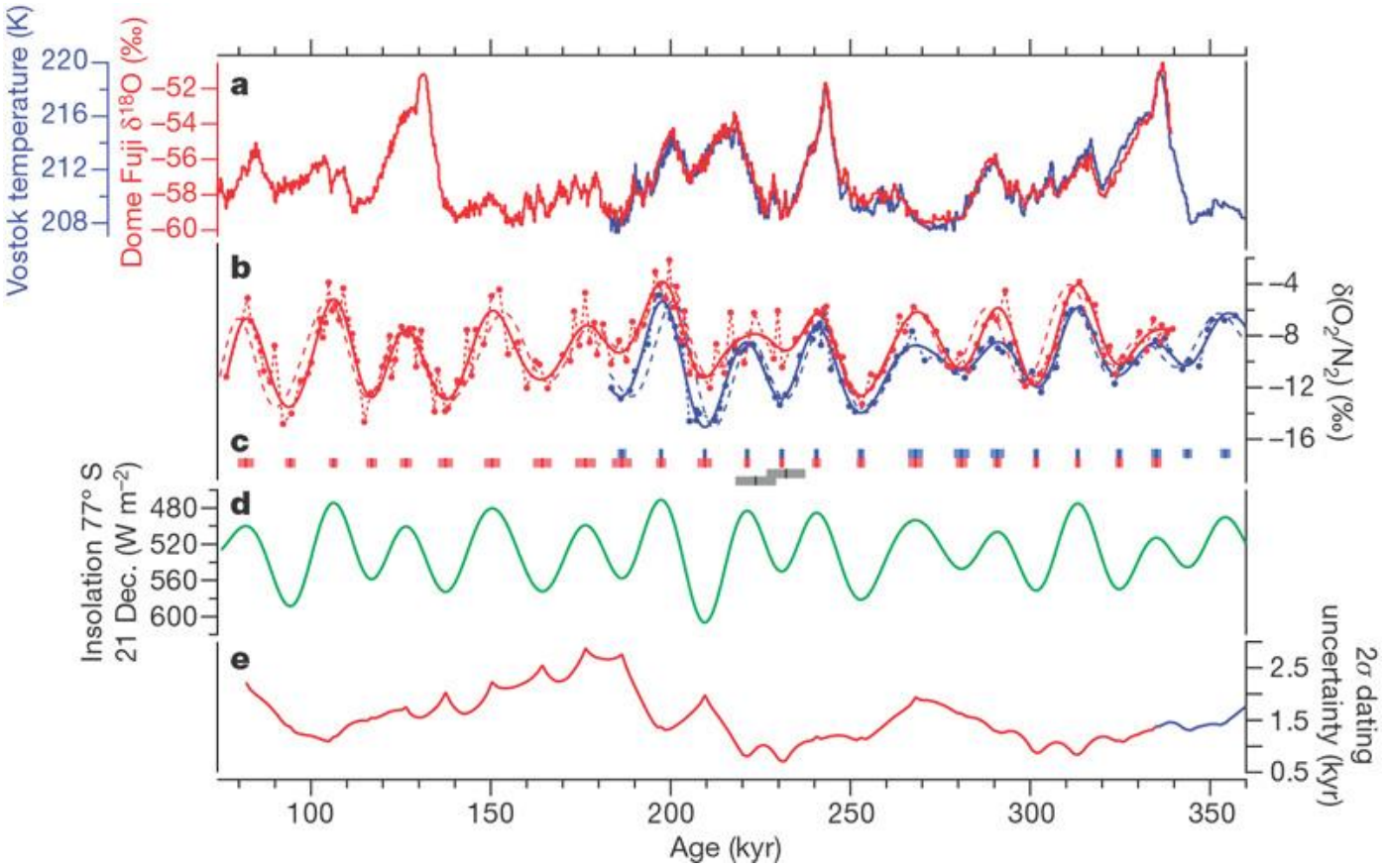

a, Dome Fuji $^{18}O_{ice}$ (red, ref. 7) and Vostok temperature[12] (blue, converted from D) on the respective O_2/N_2 timescales (DFO-2006 and VkO-2006). **b**, O_2/N_2 records of the Dome Fuji[4] (filled red circles) and Vostok[5] (filled blue circles) cores and filtered curves (solid lines) on the O_2/N_2 timescales, and filtered curves on the original glaciological timescales (dashed lines). **c**, Age tie points for the Dome Fuji (red) and Vostok (blue) cores with 2 error bars. The tie points at 221.2, 230.8 and 334.9 kyr ago for DFO-2006 are adopted from the Vostok data (see text). Two discarded points of the Dome Fuji core are shown (grey markers). **d**, Summer solstice insolation at 77° S as the tuning target (inverted axis scale). **e**, 2 dating uncertainty of DFO-2006 (red) and VkO-2006 (blue, for oldest part)

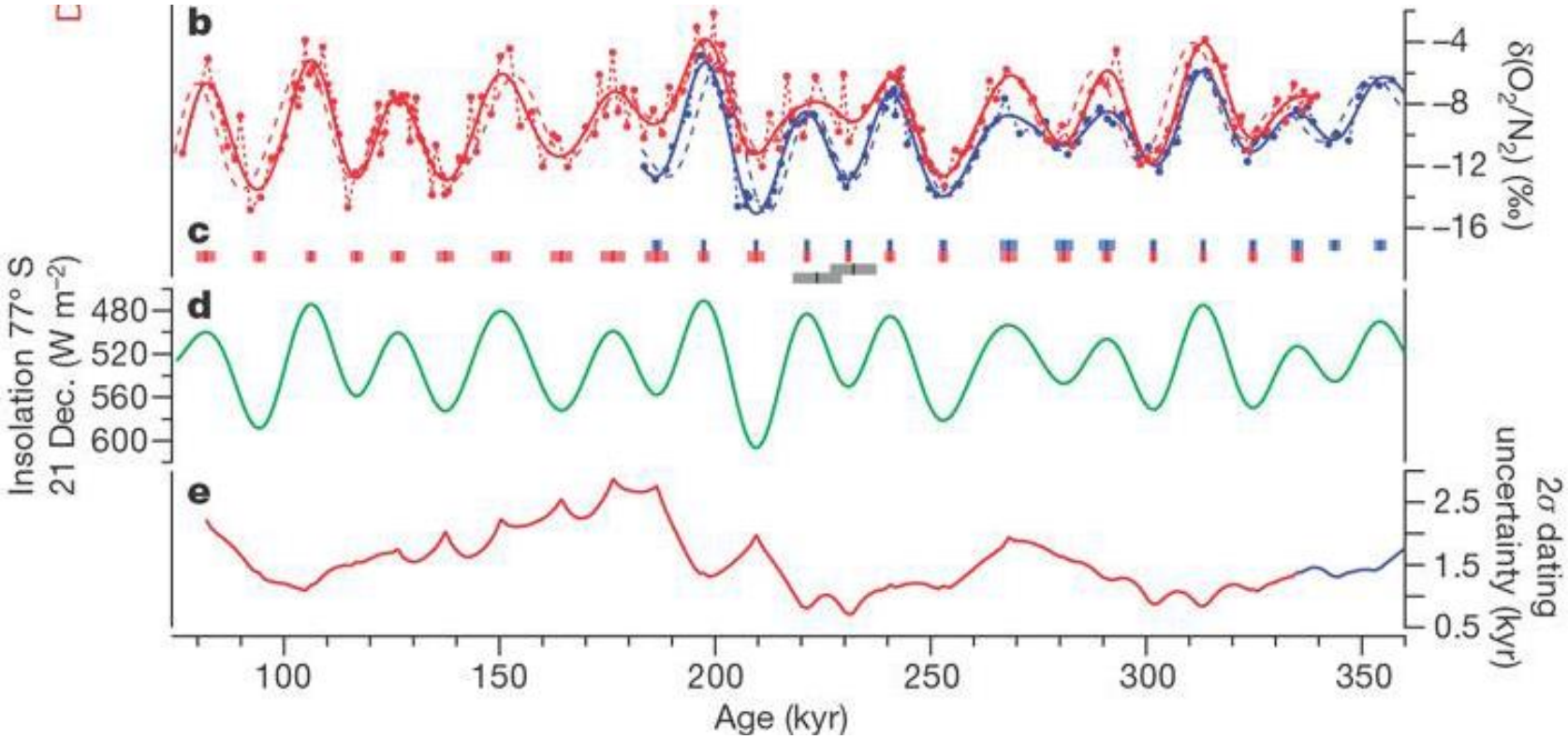

La curva verde (d) è il risultato del calcolo della insolazione massima (solstizio d'estate, 21 dicembre) tenendo conto dei moti della terra (scala invertita).
Le curve rosse e blu (b) sono il risultato della misura del delta(O_2/N_2) in due carote.
La corrispondenza delle forme permette di legare le curve sui massimi e minimi e quindi di datare I diversi strati delle carote.

E così un otteniamo un'unica scala dei tempi per tutte le grandezze misurate e che erano state datate con tecniche indipendenti. Per esempio la concentrazione di CO2. Ma anche il livello degli oceani precedentemente datato sulla base del rapporto Th/U.

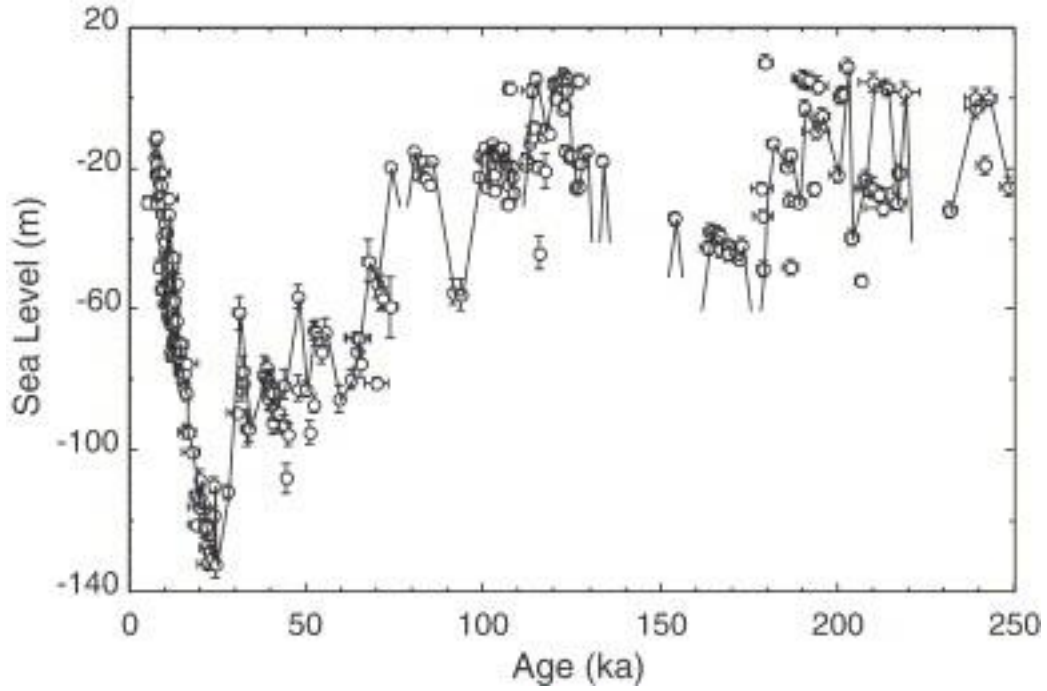

Fig. 1. A high-resolution sea-level reconstruction. Corrected coral ages have been calculated from published U and Th isotope ratio data (Bard et al., 1990a and Bard et al., 1990b; Edwards et al., 1993; Gallup et al., 1994; Bard et al., 1996; Chappell et al., ...

William G. Thompson, Steven L. Goldstein

A radiometric calibration of the SPECMAP timescale

Quaternary Science Reviews, Volume 25, Issues 23–24, 2006, 3207–3215

http://dx.doi.org/10.1016/j.quascirev.2006.02.007

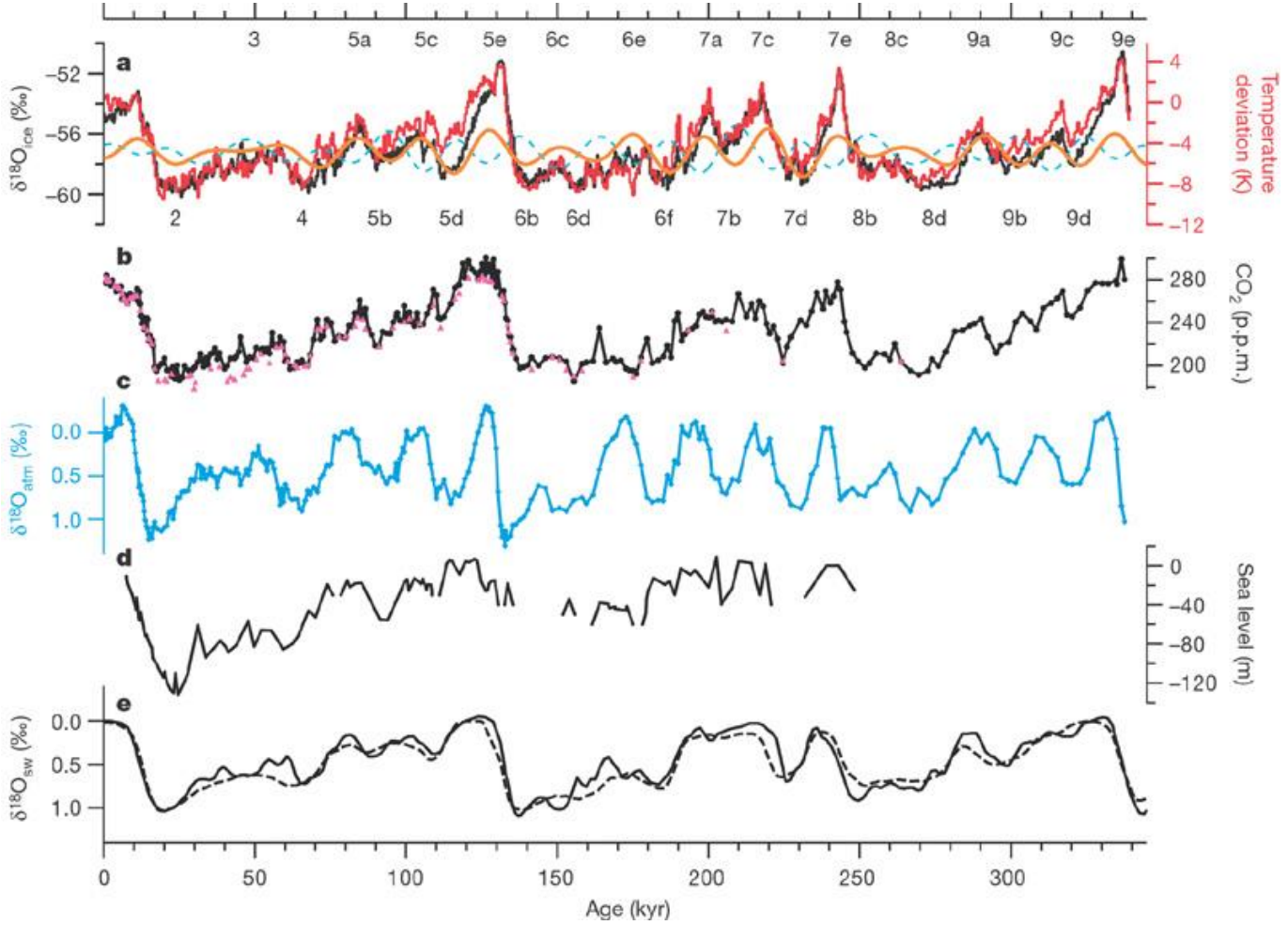

a, Dome Fuji $^{18}O_{ice}$ (black, ref. 7) and temperature deviation (T_{site}) from the mean of the last 10 kyr (red, this study) on the DFO-2006 timescale, and summer solstice insolation at 65° N (orange) and 65° S (light blue dashed line). The insolation curves are scaled to match 65° N insolation with low-pass filtered ^{18}O (not shown) for the MIS 5b–a transition. Corresponding MIS numbers[27] are shown without implying their exact timings. The T_{site} and $^{18}O_{ice}$ records are scaled to visually match the changes from the LGM to early Holocene

b, Atmospheric CO_2 concentration from the Dome Fuji core by wet extraction[8] (black circles) and dry extraction (pink triangles, this study). (Two wet-extraction CO_2 outliers[8] (at 149.8 and 365.0 m, in Holocene ice) are excluded from this plot. Experimental error rather than chemical reaction in meltwater[8] may be suspected for these samples, which were measured on the first day of 80 measurement days.) Note that the dry extraction values are too low in the transition zone from air bubbles to clathrate hydrates (for 30–55 kyr ago), and the wet-extraction values are too high in the LGM[8] (around 20 kyr ago). **c**, Dome Fuji $^{18}O_{atm}$ record (this study, inverted axis scale). **d**, Sea level reconstruction based on radiometric dating of fossil corals with open system correction[28]. **e**, Orbitally tuned $^{18}O_{sw}$ (inverted axis scale) reconstructed from isotope records of marine sediment cores through regression analyses[29] (solid line) and ice sheet modelling[30] (dashed line).

Tutte le quantità misurate:

Concentrazione di CO_2
Livello degli oceani
Rapporti isotopici dell'ossigeno in aqua marina, nel ghiaccio antartico e di quello incluso nei pori del ghiaccio. Rapporto isotopico dell'idrogeno

sono strettamente correlate all'insolazione estiva dell'emisfrero nord.

Il clima, misurato in antartide dipende dall'insolazione estiva del NORD del pianeta!

La concentrazione di CO_2 ha un ruolo importante (effetto serra).

Possiamo vedere le periodicità presenti nelle varie quantità. Ma anche gli sfasamenti (ritardi).

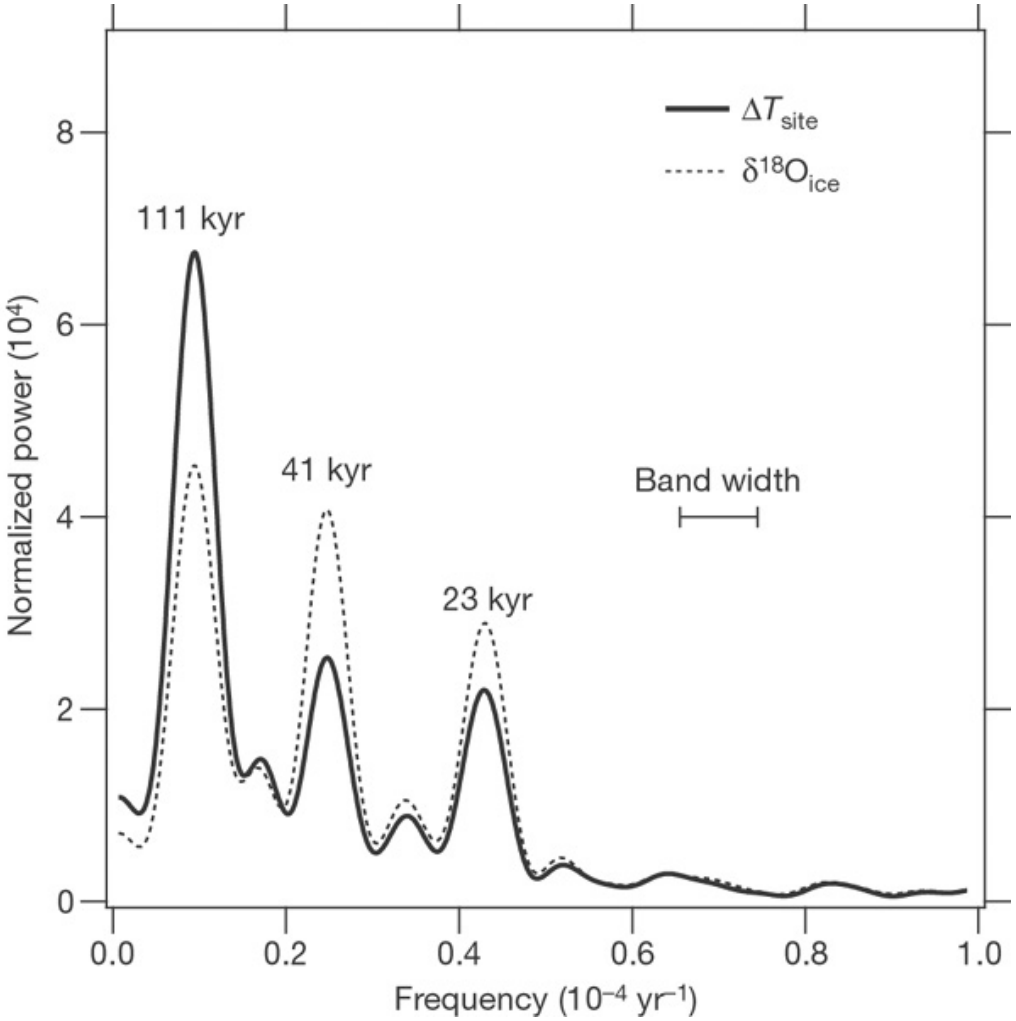

Power spectra of ^{18}O and T_{site} records calculated by the Blackman–Tukey method with 50% lags.

The $^{18}O_{ice}$ power spectrum shows strong power in the precession band (23-kyr period) with a mean lag of 1.0 0.5 kyr behind precession. The site temperature T_{site} shows smaller obliquity and precession components than $^{18}O_{ice}$, and the precession component is as strong as the obliquity component. The lag of T_{site} behind precession is 1.8 ± 0.5 kyr. At 41-kyr period, $^{18}O_{ice}$ and T_{site} lag behind obliquity by 2.1 ± 0.7 and 4.7± 1.1 kyr, respectively.

Importantly, the southern summer insolation is in anti-phase (or is completely out of phase) with Antarctic climate, so does not appear to have a strong influence on the orbital-scale Antarctic climatic changes. These phasings suggest that the Antarctic climate on orbital timescales is paced by northern summer insolation presumably through northern ice sheet variation, although minor influence by southern insolation cannot be entirely ruled out.

Another remarkable feature of the data is that the last four Antarctic terminations occur within the rising phase of northern summer insolation.
The onsets of these terminations occur 6, 3, 7 and 2 kyr later than the 65° N summer solstice insolation minima, respectively, for terminations I, II, III and IV, and the entire duration of these warmings also fit within the rising phase of northern summer insolation. The timing of the last four terminations is thus fully consistent with Milankovitch theory.

6 Ky delay

3

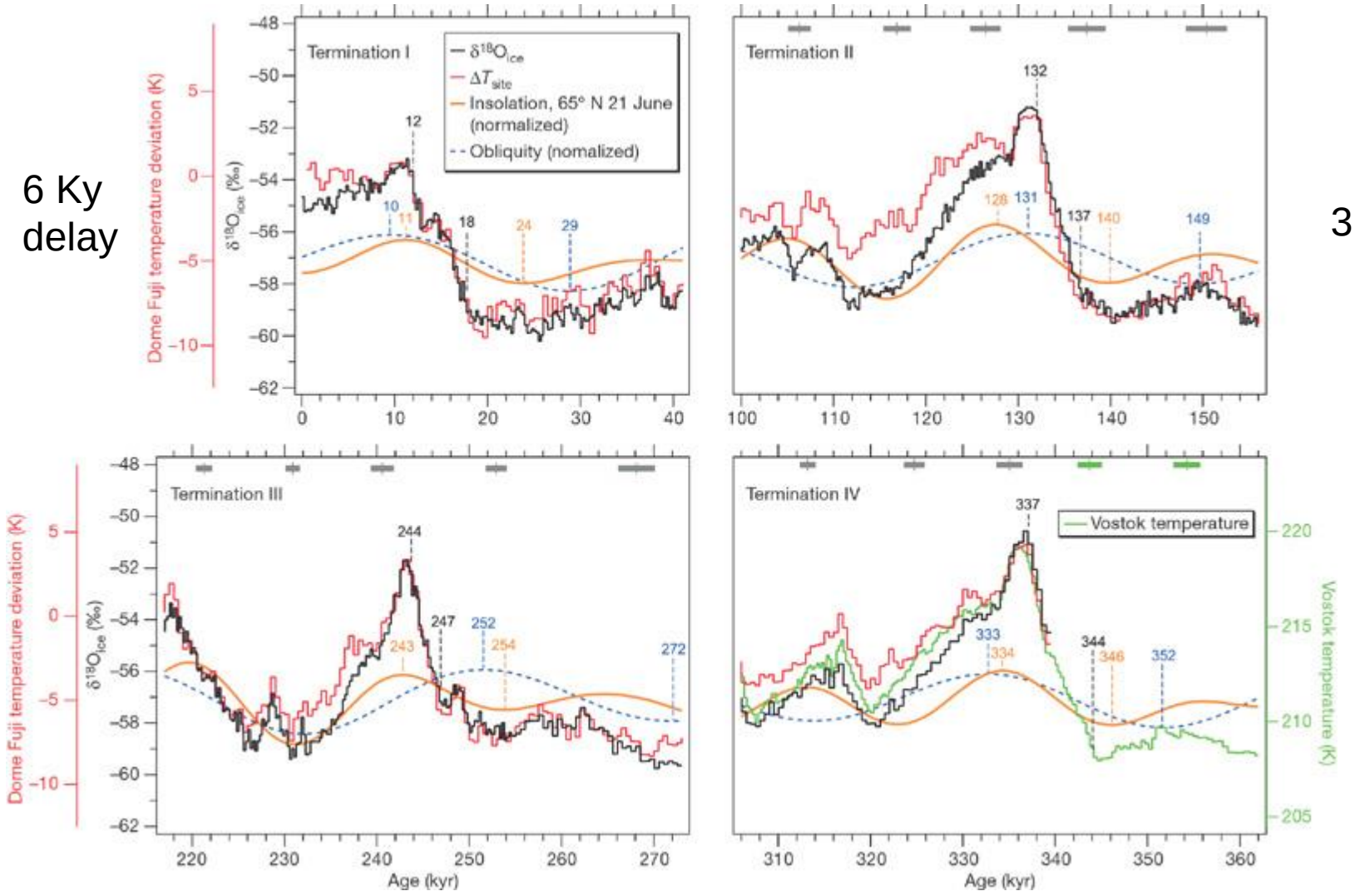

7

2

Shown are Dome Fuji $^{18}O_{ice}$ and temperature T_{site} (red, this study) on the DFO-2006 timescale compared with 65° N summer solstice insolation (orange) and obliquity (blue dashed line). The Vostok temperature[12] on the VkO-2006 timescale is also plotted for termination IV (green). Numbers indicate key timings (minima and maxima of insolation and obliquity, and onset and end of $^{18}O_{ice}$ increases). The age tie points with 2 uncertainties are shown at the top.

In summary, the mean phasing of Antarctic climate, as well as the timing of the last four terminations and three post-interglacial coolings, are consistent with the hypothesis that high northern latitude summer insolation is the trigger of glacial–interglacial cycles. The role of CO_2 as conveyor and amplifier of the orbital input should be quantified with climate models run using our new timescale; this quantification is important for future climate change predictions.

Problemi aperti? MOLTI!
In particolare, l'analisi isotopica mostra come la periodicità dominante della risposta climatica sia di circa 100.000 anni (eccentricità dell'orbita?), mentre ci si aspetterebbe che precessione e inclinazione debbano essere più importanti.

Inclinazione orbitale

L'inclinazione orbitale terrestre misurata rispetto ad un piano di riferimento (ad esempio, al piano equatoriale del Sole) è soggetta ad oscillazioni periodiche. Milankovitch non studiò però questo movimento tridimensionale.
Ricercatori di epoca più recente notarono questa variazione e notarono che l'orbita si muove rispetto alle orbite degli altri pianeti. Il piano invariante, il piano che rappresenta il momento angolare del sistema solare, è circa equivalente al piano orbitale di Giove. L'inclinazione dell'orbita terrestre rispetto al piano invariante oscilla con un periodo di 100.000 anni, coincidendo quasi con il ciclo delle glaciazioni.
È stato ipotizzato che vi sia un disco di polvere ed altri detriti nel piano invariante, che influenza il clima terrestre in vari modi. La Terra attualmente attraversa questo piano attorno al 9 gennaio e il 9 luglio, quando vi è un aumento delle meteore rilevate dai radar e delle nuvole nottilucenti legate ad esse.

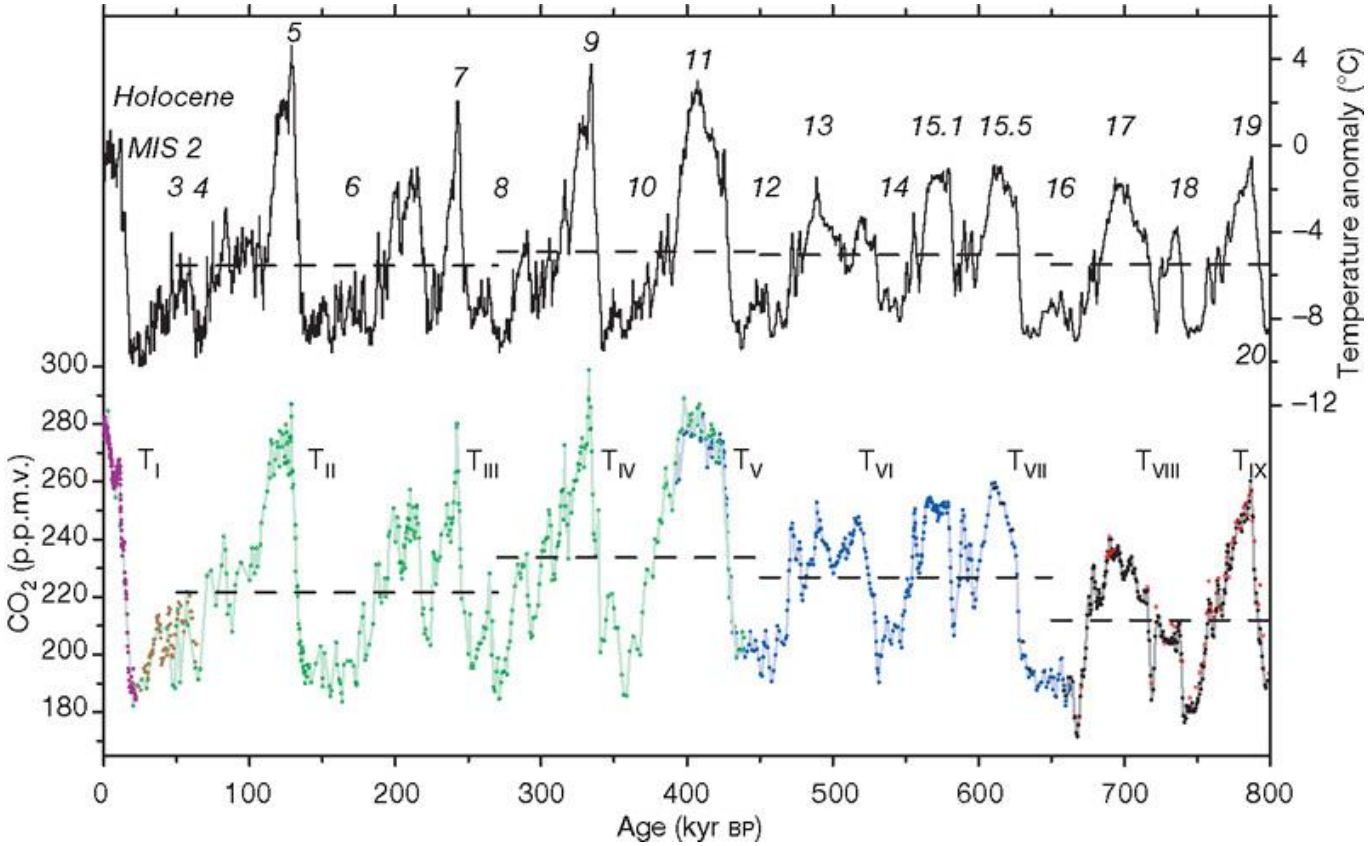

Compilation of CO_2 records and EPICA Dome C temperature anomaly over the past 800 kyr. High-resolution carbon dioxide concentration record 650,000–800,000 years before present. D. Lüthi et al., Nature 453, 379-382(15 May 2008)

The Dome C temperature anomaly record with respect to the mean temperature of the last millennium[8] (based on original deuterium data interpolated to a 500-yr resolution), plotted on the EDC3 timescale[13], is given as a black step curve. Data for CO_2 are from Dome C (solid circles in purple[5], blue[4], black: this work, measured at Bern; red open circles: this work, measured at Grenoble), Taylor Dome[6] (brown) and Vostok[1, 2, 3] (green). All CO_2 values are on the EDC3_gas_a age scale[26]. Horizontal lines are the mean values of temperature and CO_2 for the time periods 799–650, 650–450, 450–270 and 270–50 kyr bp. Glacial terminations are indicated using Roman numerals in subscript (for example T_I); Marine Isotope Stages (MIS) are given in italic Arabic numerals[27].

Methane records and EPICA/Dome C D. Orbital and millennial-scale features of atmospheric CH_4 over the past 800,000 years

L.Loulergue et al. Nature 453, 383-386(15 May 2008)

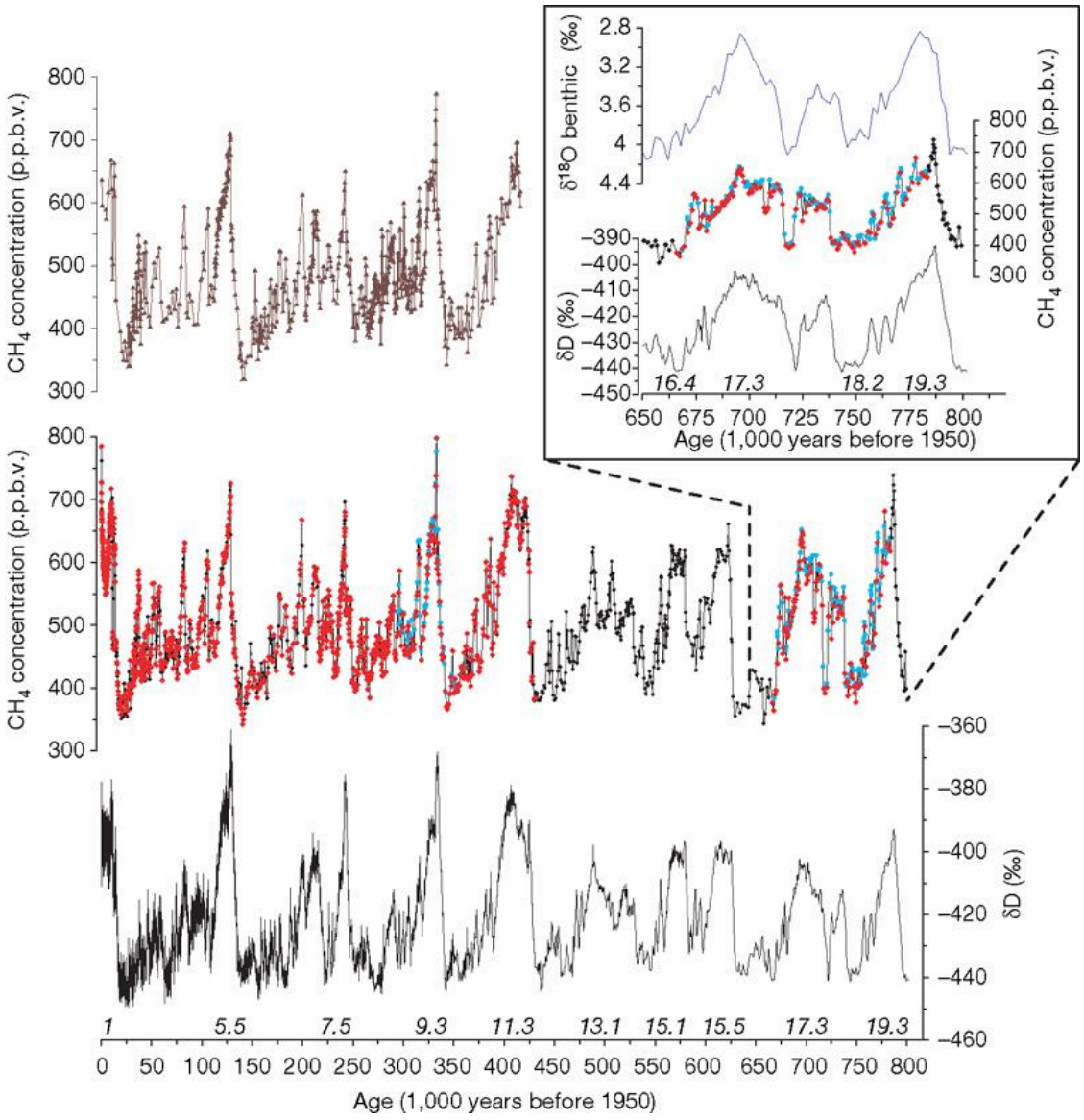

Bottom to top: D record[9]; EDC methane record (previously published data[2], black diamonds; new data from LGGE, red diamonds; new data from Bern, blue dots); Vostok methane record[1]. Marine Isotope Stage numbering is given at the bottom of each interglacial. Insert: expanded view of the bottom section of EDC: D values[9] (black line), CH_4 (black line) from EDC and stack benthic ^{18}O values (blue line)[19] for the period from MIS 16 to 20.2, on their respective age scales. $^{18}O = [(^{18}O/^{16}O)_{sample}/(^{18}O/^{16}O)_{standard}] - 1$, where standard is vPDB; $D = [(D/H)_{sample}/(D/H)_{standard}] - 1$ where standard is SMOW.

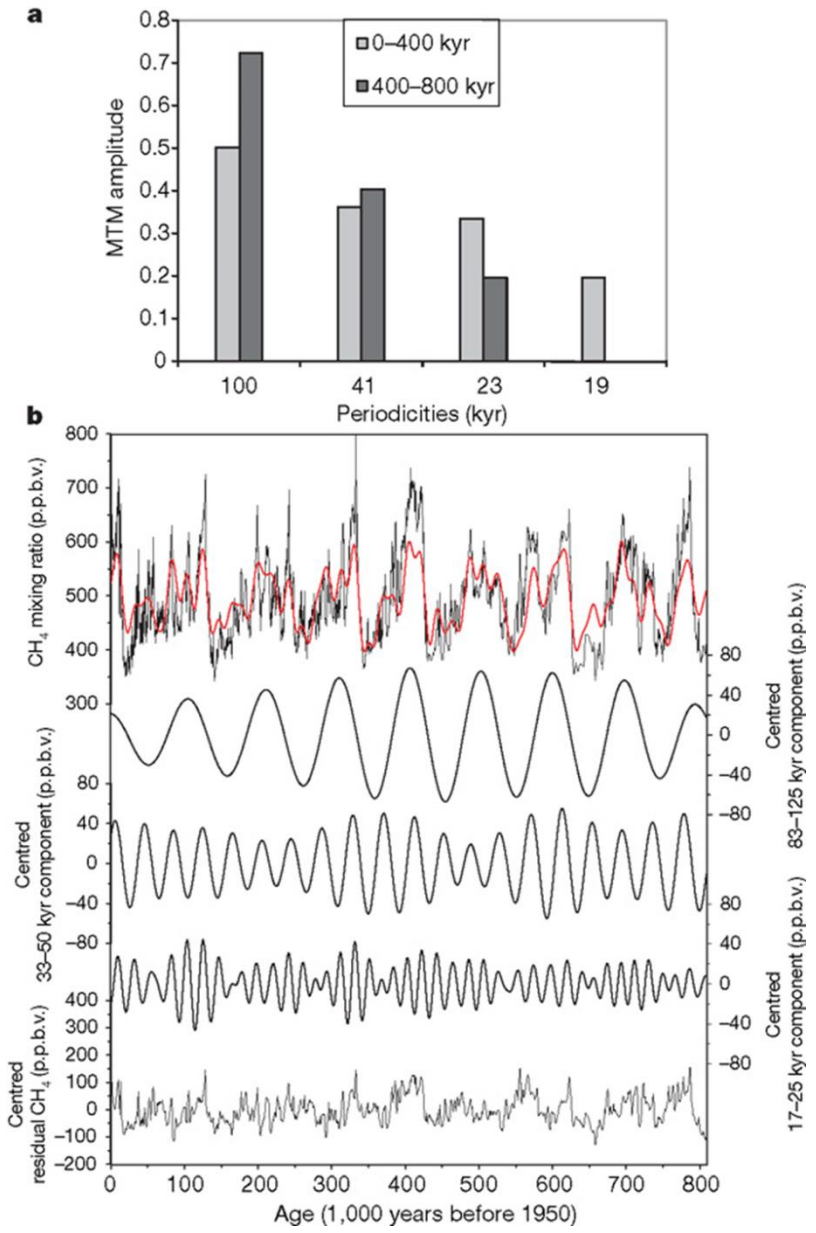

a, Amplitude of orbital periodicities in the methane record for the time ranges 0–400 kyr and 400–800 kyr, using the multi-taper method (MTM) with normalized data. The 19-kyr component is absent at 400–800 kyr because of its statistical non-significance (*F*-test <0.95, see Supplementary Information). **b**, Orbital components and residuals (expressed in p.p.b.v. on the centred signal) of the CH_4 record over the past 800 kyr. The red line combines the three periodicities. Note that the amplitude of the orbital components and residuals is similar (200 p.p.b.v.). The residual CH_4 signal contains other statistically significant periodicities at 4.8 and 8.7 kyr and another periodicity at 10–11 kyr slightly below the confidence limit, not discussed here.

Atmospheric methane is an important greenhouse gas and a sensitive indicator of climate change and millennial-scale temperature variability[1]. Its concentrations over the past 650,000 years have varied between 350 and 800 parts per 10^9 by volume (p.p.b.v.) during glacial and interglacial periods, respectively[2]. In comparison, present-day methane levels of 1,770 p.p.b.v. have been reported[3]. Insights into the external forcing factors and internal feedbacks controlling atmospheric methane are essential for predicting the methane budget in a warmer world[3]. Here we present a detailed atmospheric methane record from the EPICA Dome C ice core that extends the history of this greenhouse gas to 800,000 yr before present. The average time resolution of the new data is 380 yr and permits the identification of orbital and millennial-scale features. Spectral analyses indicate that the long-term variability in atmospheric methane levels is dominated by 100,000 yr glacial–interglacial cycles up to 400,000 yr ago with an increasing contribution of the precessional component during the four more recent climatic cycles. We suggest that changes in the strength of tropical methane sources and sinks (wetlands, atmospheric oxidation), possibly influenced by changes in monsoon systems and the position of the intertropical convergence zone, controlled the atmospheric methane budget, with an additional source input during major terminations as the retreat of the northern ice sheet allowed higher methane emissions from extending periglacial wetlands. Millennial-scale changes in methane levels identified in our record as being associated with Antarctic isotope maxima events[1, 4] are indicative of ubiquitous millennial-scale temperature variability during the past eight glacial cycles.

Come si costruisce la cronologia della carota?
Bisogna costruire una tabella di corrispondenza tra profondità (misurata in metri) ed età (misurata in migliaia di anni)

Gas is trapped in polar ice sheets at ~50-120m below the surface and is therefore younger than the surrounding ice. Firn densification models are used to evaluate this ice age-gas age difference (Delta age) in the past. However, such models need to be validated by data, in particular for periods colder than present day on the East Antarctic plateau. Here we bring new constraints to test a firn densification model applied to the EPICA Dome C (EDC) site for the last 50 kyr, by linking the EDC ice core to the EPICA Dronning Maud Land (EDML) ice core, both in the ice phase (using volcanic horizons) and in the gas phase (using rapid methane variations). We also use the structured 10Be peak, occurring 41 kyr before present (BP) and due to the low geomagnetic field associated with the Laschamp event, to experimentally estimate the Delta age during this event.

Come si costruisce la cronologia della carota?
Bisogna costruire una tabella di corrispondenza tra profondità (misurata in metri) ed età (misurata in migliaia di anni)

Clim. Past, 3, 485–497, 2007
www.clim-past.net/3/485/2007/

Climate of the Past

The EDC3 chronology for the EPICA Dome C ice core

F. Parrenin[1], J.-M. Barnola[1], J. Beer[2], T. Blunier[3], E. Castellano[4], J. Chappellaz[1], G. Dreyfus[5], H. Fischer[6], S. Fujita[7], J. Jouzel[5], K. Kawamura[8], B. Lemieux-Dudon[1], L. Loulergue[1], V. Masson-Delmotte[5], B. Narcisi[9], J.-R. Petit[1], G. Raisbeck[10], D. Raynaud[1], U. Ruth[6], J. Schwander[3], M. Severi[4], R. Spahni[3], J. P. Steffensen[11], A. Svensson[11], R. Udisti[4], C. Waelbroeck[1], and E. Wolff[12]

[1]Laboratoire de Glaciologie et Géophysique de l'Environnement, CNRS and Joseph Fourier University, Grenoble, France
[2]Department of Surface Waters, EAWAG, Dübendorf, Switzerland
[3]Climate and Environmental Physics, Physics Institute, University of Bern, Bern, Switzerland
[4]Department of Chemistry, University of Florence, Florence, Italy
[5]Laboratoire des Sciences du Climat et de l'Environnement, IPSL/CEA/CNRS/UVSQ, Gif-Sur-Yvette, France
[6]Alfred-Wegener-Institute for Polar and Marine Research, Bremerhaven, Germany
[7]National Institute of Polar Research, Research Organization of Information and Systems (ROIS), Tokyo, Japan
[8]Center for Atmospheric and Oceanic Studies Graduate School of Science, Tohoku University, Sendai, Japan
[9]ENEA, C. R. Casaccia, Roma, Italy
[10]CSNSM/IN2P3/CNRS, Orsay, France
[11]Niels Bohr Institute, University of Copenhagen, Copenhagen, Denmark
[12]British Antarctic Survey, Cambridge, UK

Table 1. Age markers used for the construction of the EDC3 age scale. They fall into 3 categories: 1) Age markers used to control the poorly known parameters of the modelling; 2) Age markers used for a posteriori correction in the top part of the core (EDC3 is required to pass exactly through those age markers); 3) Age markers used to correct for ice flow anomalies in the bottom part.

age marker	depth (m)	age (kyr BP)	error bar (kyr BP)	model control	top correction	bottom correction
Krakatua	8.35	0.066	0.001		X	
Tambora	12.34	0.134	0.001		X	
Huaynaputina	23.20	0.349	0.001		X	
Kuwae	29.27	0.492	0.005		X	
El Chichon?	38.12	0.691	0.005	X	X	
Unidentified	39.22	0.722	0.006		X	
Unknown	41.52	0.779	0.006		X	
$^{10}Be/^{14}C$	107.83	2.716	0.05	X		
$^{10}Be/^{14}C$	181.12	5.28	0.05	X	X	
YD/Holocene	361.5	11.65	0.18	X		
PB/BO	427.2	15.0	0.24	X	X	
^{10}Be peak	740.08	41.2	1	X	X	
Mt Berlin erupt.	1265.10	92.5	2	X		
term. II	1698.91	130.1	2	X		
air content	1082.34	70.6	4	X		
air content	1484.59	109.4	4	X		
air content	1838.09	147.6	4	X		
air content	2019.73	185.3	4	X		
air content	2230.71	227.3	4	X		
air content	2387.95	270.4	4	X		
air content	2503.74	313.4	4	X		
air content	2620.23	352.4	4	X		
air content	2692.69	390.5	4	X		
air content	2789.58	431.4	4	X		
$^{18}O_{atm}$	2714.32	398.4	6			X
$^{18}O_{atm}$	2749.04	408.6	6			X
$^{18}O_{atm}$	2772.27	422.0	6			X
$^{18}O_{atm}$	2799.36	441.0	6			X
$^{18}O_{atm}$	2812.69	454.3	6			X
$^{18}O_{atm}$	2819.2	464.6	6			X
$^{18}O_{atm}$	2829.36	474.8	6			X
$^{18}O_{atm}$	2841.75	485.3	6			X
$^{18}O_{atm}$	2856.27	495.9	6			X
$^{18}O_{atm}$	2872.56	506.6	6			X
$^{18}O_{atm}$	2890.33	517.6	6			X
$^{18}O_{atm}$	2913.3	532.0	6			X
$^{18}O_{atm}$	2921.99	545.3	6			X
$^{18}O_{atm}$	2938.24	556.4	6			X
$^{18}O_{atm}$	2968.08	567.6	6			X
$^{18}O_{atm}$	2998.96	578.6	6	X		X
$^{18}O_{atm}$	3008.93	589.5	6			X
$^{18}O_{atm}$	3017.25	600.1	6			X
$^{18}O_{atm}$	3027.54	610.9	6			X
$^{18}O_{atm}$	3035.41	622.1	6	X		X
$^{18}O_{atm}$	3043.01	634.4	6			X
$^{18}O_{atm}$	3048.51	649.1	6			X
$^{18}O_{atm}$	3056.77	660.8	6			X
$^{18}O_{atm}$	3065.93	671.7	6			X
$^{18}O_{atm}$	3077.74	682.3	6			X
$^{18}O_{atm}$	3093.51	693.2	6			X
$^{18}O_{atm}$	3112.43	704.0	6			X
$^{18}O_{atm}$	3119.57	714.4	6			X
$^{18}O_{atm}$	3124.27	724.4	6			X
$^{18}O_{atm}$	3136.18	733.9	6			X
$^{18}O_{atm}$	3143.2	741.9	6			X
$^{18}O_{atm}$	3152.25	749.2	6			X
$^{18}O_{atm}$	3158.91	758.1	6			X
$^{18}O_{atm}$	3166.87	767.7	6			X
$^{18}O_{atm}$	3174.81	777.6	6			X
$^{18}O_{atm}$	3180.6	787.7	6			X
$^{18}O_{atm}$	3189.83	797.5	6			X
B-M reversal	3165	785	20	X		

Table 1. Age markers used for the construction of the EDC3 age scale. They fall into 3 categories: 1) Age markers used to control the poorly known parameters of the modelling; 2) Age markers used for a posteriori correction in the top part of the core (EDC3 is required to pass exactly through those age markers); 3) Age markers used to correct for ice flow anomalies in the bottom part.

age marker	depth (m)	age (kyr BP)	error bar (kyr BP)	model control	top correction	bottom correction
Krakatua	8.35	0.066	0.001		X	
Tambora	12.34	0.134	0.001		X	
Huaynaputina	23.20	0.349	0.001		X	
Kuwae	29.27	0.492	0.005		X	
El Chichon?	38.12	0.691	0.005	X	X	
Unidentified	39.22	0.722	0.006		X	
Unknown	41.52	0.779	0.006		X	
$^{10}Be/^{14}C$	107.83	2.716	0.05	X		
$^{10}Be/^{14}C$	181.12	5.28	0.05	X	X	
YD/Holocene	361.5	11.65	0.18	X		
PB/BO	427.2	15.0	0.24	X	X	
^{10}Be peak	740.08	41.2	1	X	X	
Mt Berlin erupt.	1265.10	92.5	2	X		
term. II	1698.91	130.1	2	X		
air content	1082.34	70.6	4	X		
air content	1484.59	109.4	4	X		
air content	1838.09	147.6	4	X		
air content	2019.73	185.3	4	X		
air content	2230.71	227.3	4	X		
air content	2387.95	270.4	4	X		
air content	2503.74	313.4	4	X		
air content	2620.23	352.4	4	X		
air content	2692.69	390.5	4	X		
air content	2789.58	431.4	4	X		
$^{18}O_{atm}$	2714.32	398.4	6			X
$^{18}O_{atm}$	2749.04	408.6	6			X
$^{18}O_{atm}$	2772.27	422.0	6			X
$^{18}O_{atm}$	3174.81	777.6	6			X
$^{18}O_{atm}$	3180.6	787.7	6			X
$^{18}O_{atm}$	3189.83	797.5	6			X
B-M reversal	3165	785	20	X		

Abstract. The EPICA (European Project for Ice Coring in Antarctica) Dome C drilling in East Antarctica has now been completed to a depth of 3260 m, at only a few meters above bedrock. Here we present the new EDC3 chronology, which is based on the use of 1) a snow accumulation and mechanical flow model, and 2) a set of independent age markers along the core. These are obtained by pattern matching of recorded parameters to either absolutely dated paleoclimatic records, or to insolation variations. We show that this new time scale is in excellent agreement with the Dome Fuji and Vostok ice core time scales back to 100 kyr within 1 kyr. Discrepancies larger than 3 kyr arise during MIS 5.4, 5.5 and 6, which points to anomalies in either snow accumulation or mechanical flow during these time periods. We estimate that EDC3 gives accurate event durations within 20% (2σ) back to MIS11 and accurate absolute ages with a maximum uncertainty of 6 kyr back to 800 kyr.

MIS marine isotope stages

MIS 1 - 14 kya
MIS 2 - 29 near Last Glacial Maximum
MIS 3 - 57[a]
MIS 4 - 71
MIS 5 - 130, usually sub-divided into a to e:
- MIS 5a - 82
- MIS 5b - 87
- MIS 5c - 96
- MIS 5d - 109
- MIS 5e - 123 (Eemian or Ipswichian)

MIS 6 - 191
MIS 7 - 243 (Aveley)
MIS 8 - 300
MIS 9 - 337 (informally called the Purfleet Interglacial)[15]
MIS 10 - 374
MIS 11 424 (Hoxnian Stage in Britain)
MIS 12 - 478 (Anglian Stage in Britain)
MIS 13 - 533
MIS 14 - 563
MIS 15 - 621
MIS 16 - 676
MIS 17 - 712
MIS 18 - 761
MIS 19 - 790
MIS 20 - 814

In the absence of radiochronologic constraints, numerous methods have been developed to date ice cores. They fall into 4 categories: (1) counting of layers representing a known time interval, e.g. annual layers, (2) ice flow modelling, (3) wiggle matching on other precisely dated time series, in particular insolation variations, and (4) use of climate independent age markers, like volcanic eruptions.

All the above dating methods have advantages and drawbacks. Layer counting (Andersen et al., 2007) and ice flow modelling (Parrenin et al., 2006) are accurate in terms of event durations because they are based on the evaluation of the annual layer thickness. On the other hand, errors cumulate and the accuracy on absolute ages decreases with depth.

The new layer-counted chronology for Greenland (GICC05, Vinther et al., 2006; Rasmussen et al., 2006; Andersen et al., 2006; Svensson et al., 2006) uses an improved multi-parameter counting approach, and currently extends back to around 42 kyr BP with a maximum counting error of 4 to 7% during the last glacial period. Unfortunately, layer counting is not feasible in central Antarctica where annual cycles are barely distinguishable (Ekaykin et al., 2002).

Comparison of paleoclimatic records to insolation variations (so-called orbital tuning methods) are generally applicable to a whole ice core, as long as the stratigraphy is preserved (e.g., Martinson et al., 1987; Dreyfus et al., 2007). On the other hand: (1) the accuracy in terms of event durations is poor, (2) the accuracy in terms of absolute ages is limited by the hypothesis of a constant phasing between the climatic record used for the orbital tuning procedure and the insolation variations (and, by definition, does not allow one to infer this phasing). The advantage is that the achieved accuracy does not decrease with depth (assuming the underlying mechanism stays constant). As a consequence, it is currently the most precise method to date the bottom of deep ice cores.

Recently, the search for local insolation proxies in ice cores as, e.g. the O_2/N_2 ratio (Bender et al., 2002; Kawamura et al., 2007) or the air content record (Raynaud et al., 2007) has opened new prospects for eliminating the reliance on this hypothesis of constant insolation/climate phase, potentially allowing an accuracy within 1 kyr to be achieved in the coming years.

Precisely dated volcanic horizons provide important age markers. This is the case for the last millenium (Traufetter et al., 2004), but beyond that limit, only a few of them have accurate absolute ages (Narcisi et al., 2006). In Antarctic ice cores, comparison to absolutely dated paleoclimatic records is particularly relevant for the dating of the D-O events, which have been accurately dated in several archives, and whose rapid transitions can be localized with a high accuracy in the Antarctic CH_4 record. The transfer of those age markers to the Antarctic ice matrix requires the evaluation of the ice/gas age difference with a firn densification model (e.g., Goujon et al., 2003, and references therein).

Dansgaard-Oeschger (D-O)

Dansgaard–Oeschger events (often abbreviated **D–O events**) are rapid climate fluctuations that occurred 25 times during the last glacial period. Some scientists (see below) claim that the events occur quasi-periodically with a recurrence time being a multiple of 1,470 years, but this is debated. The comparable climate cyclicity during the Holocene is referred to as Bond events.

Temperature proxy from four ice cores for the last 140,000 years, clearly indicating the greater magnitude of the D-O effect in the northern hemisphere

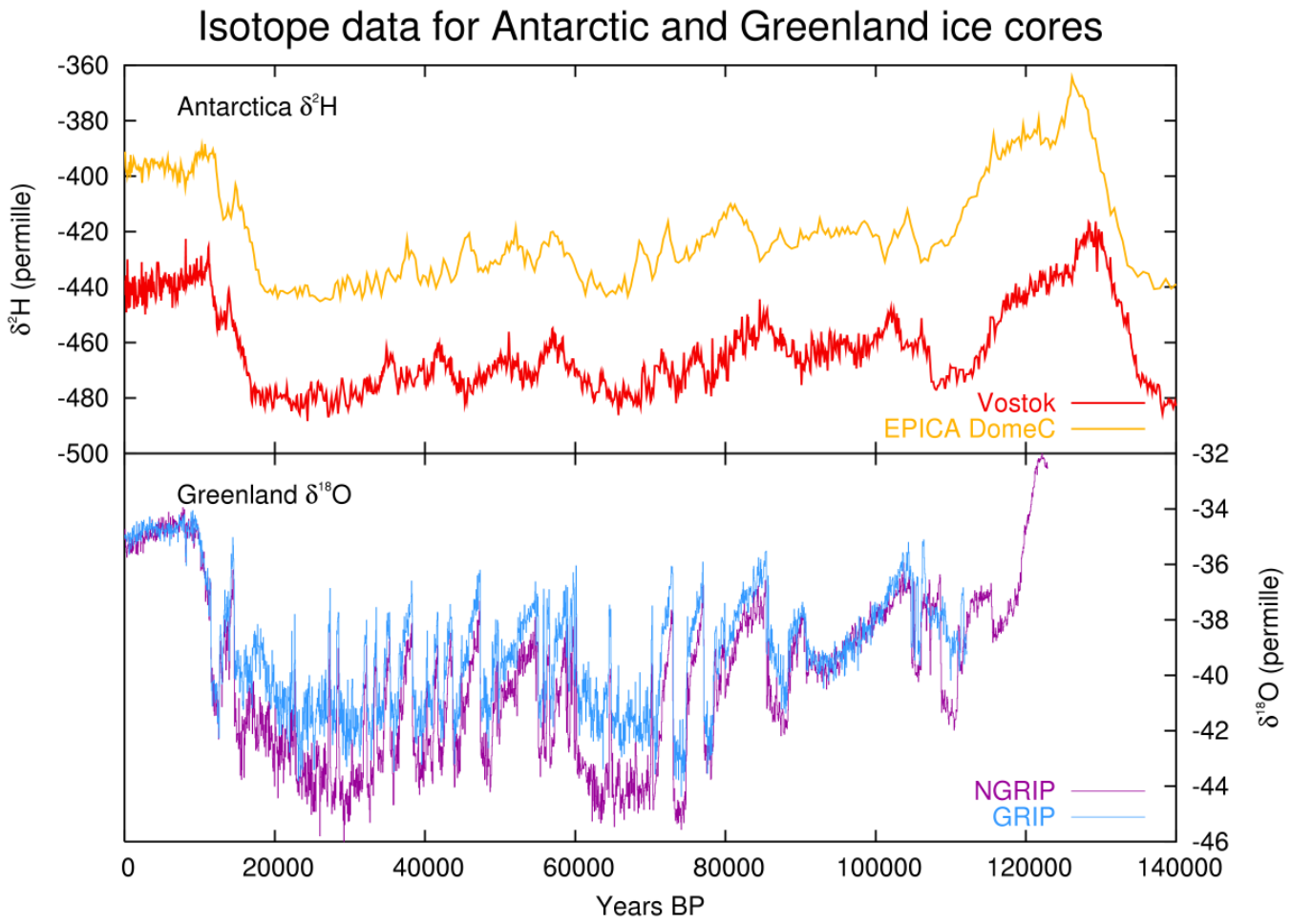

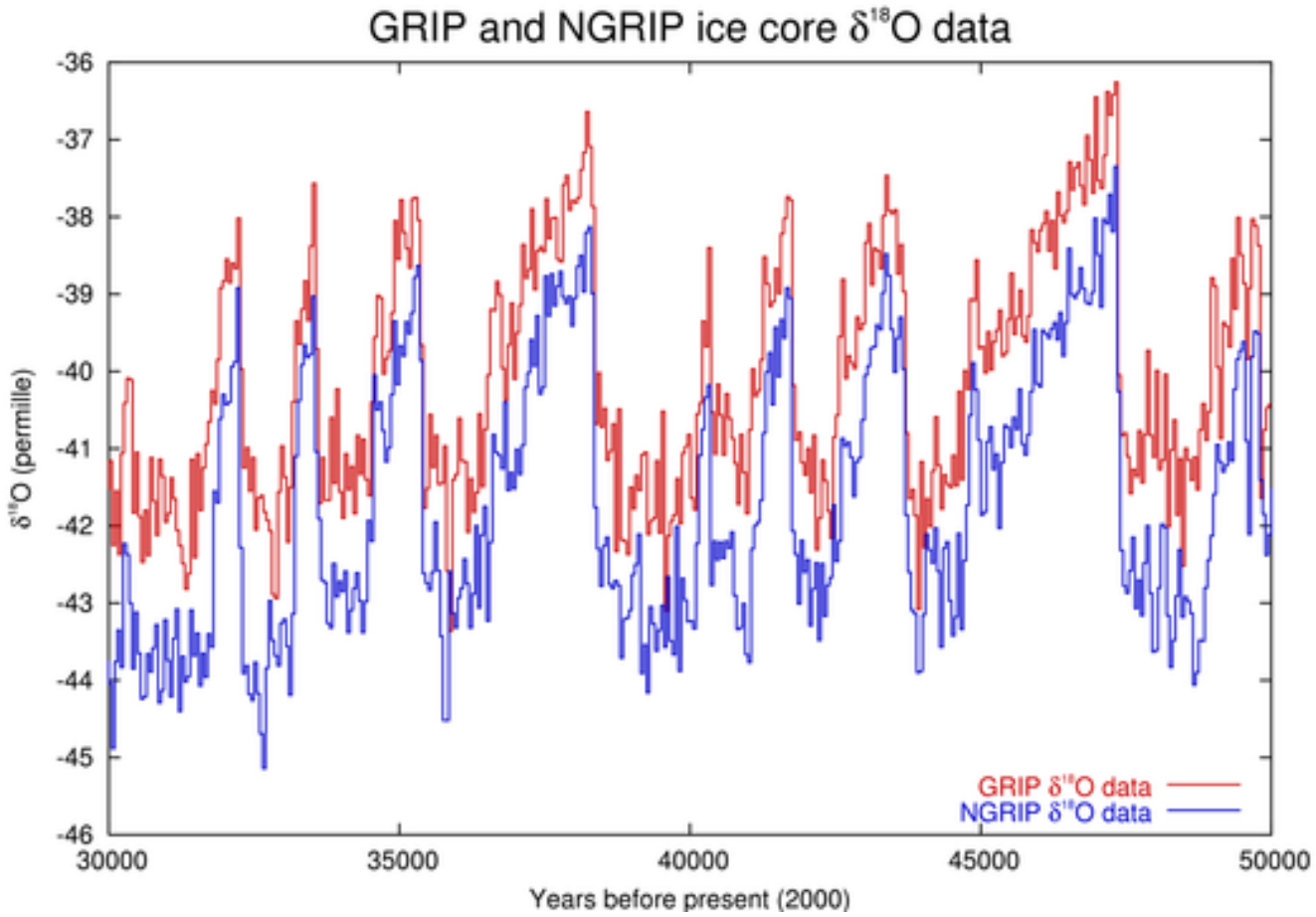

A closeup near 40 kyr BP, showing reproducibility between cores

In the Northern Hemisphere, they take the form of rapid warming episodes, typically in a matter of decades, each followed by gradual cooling over a longer period.

The course of a D-O event sees a rapid warming of temperature, followed by a cool period lasting a few hundred years. This cold period sees an expansion of the polar front, with ice floating further south across the North Atlantic ocean.

2.1 Dated volcanic eruptions during the last millenium

Using sulphate data (Castellano et al., 2005), several volcanic eruptions of known age have been identified in the EDC96 ice core during the Holocene. Among these, only a few of the most recent are independently absolutely dated (Traufetter et al., 2004): Krakatau[1], 8.35 m, AD1884±1; Tambora, 12.34 m, AD1816±1; Huaynaputina, 23.20 m, AD1601±1; Kuwae, 29.77 m, AD1460±5; Unknown (El Chichon?), 38.12 m, AD1259±5; Unidentified, 39.22 m, AD1228±5; Unknown, 41.52 m, AD1171±6.

2.2 Synchronisation onto GICC05 and INTCAL with ^{10}Be for the last 6 kyr

^{10}Be and ^{14}C are cosmogenic radionuclides, and their production rates are modulated by solar activity and by the strength of the Earth's magnetic field. Therefore ^{10}Be records in Greenland and Antarctica, as well as atmospheric ^{14}C reconstructions (INTCAL, Reimer et al., 2004) show common variations.

2.4 Match to GICC05 during the Laschamp event

The Laschamp geomagnetic excursion gives rise to a structured peak in the ^{10}Be records from Greenland (Yiou et al., 1997) and Antarctica (Raisbeck et al., 2002), which can be used to synchronise EDC96 to GRIP (Raisbeck et al., 2007), and in turn, to NGRIP dated by layer counting (GICC05, Andersen et al., 2006; Svensson et al., 2006). Two of the ^{10}Be sub-peaks have been localized in the EDC96 ice core at 735.35 m and 744.81 m, and at 2231.9 m and 2246.2 m at GRIP. The corresponding GICC05 age for the middle of these two peaks is 41 200 yr BP (max counting error of 1627 yr), corresponding to a depth of 740.08 m at EDC (Raisbeck et al., 2002) and we adopt this age.

This age of the Laschamp event is compatible (within the uncertainties) with K-Ar and ^{40}Ar-^{39}Ar ages from contemporaneous lava flow (40.4±2.0 kyr BP, Guillou et al., 2004). During this time period, which corresponds to D-O event 10 (Yiou et al., 1997; Raisbeck et al., 2002), GICC05 is also in good agreement with the Hulu Cave U-Th chronology (41.4 kyr BP, Wang et al., 2001), and with the Cariaco basin record (Hughen et al., 2004) when its ^{14}C ages are calibrated following the Fairbanks et al. (2005) curve (we obtain again an age of 41.2 kyr BP for the middle of the ^{10}Be peak corresponding to the middle of D-O 10). Genty et al. (2003) also found a compatible U-Th age of 40.0 kyr BP for the middle of D-O 10, though the identification of D-O 10 in this record is more ambiguous.

2.5 The Mont Berlin ash layer

Thanks to geochemical data (major elements and trace elements), Narcisi et al. (2006) identified a volcanic ash layer originating from a Mt Berlin (Antarctica) eruption. This event has been dated at 92.5±2 kyr BP by an Ar/Ar method applied on ash material collected close to the volcano.

2.3 Match to GICC05 with CH_4 during the last deglaciation

During the last deglaciation, synchronisation to the NGRIP GICC05 chronology (Rasmussen et al., 2006) is possible with the transitions (Björck et al., 1998) that are common to the Greenland and Antarctic high resolution methane records, and the Greenland climate record (Severinghaus and Brook, 1999): GS-2a/GI-1e (Oldest Dryas/Bølling), GI-1a/GS-1 (Allerød/Younger Dryas) and GS-1/Holocene (Younger Dryas/Holocene). In that way an age for the CH_4 transitions can be obtained. This age for the gas record then has to be transferred to an age for the ice. However, the uncertainty in the estimation of this age difference (Δage) is large at EDC because of the low accumulation rate and the low temperature (typical model estimates of Δage at EDC are 2200 yr for the Holocene and 5500 yr for the LGM).

2.6 Timing of termination II

The age of the rapid CH_4 event marking the end of termination II can be found by comparison to U-Th dated speleothem records, assuming that these fast transitions are synchronous. We obtain 129.3 kyr BP from Dongge cave in China (Yuan et al., 2004), and 130.9 kyr BP from Pekiin cave in Northern Israel (Bar-Matthews et al., 2003). We took the average of these two ages (130.1 kyr BP) and assumed a confidence interval of 2 kyr. We used the Δdepth estimate from the EDC2 age scale to export the CH_4 depth of 1723 m to an ice depth of 1699 m on EDC99. The uncertainty introduced by this ice/gas depth difference evaluation is only a few hundred years, so it is negligible compared to the uncertainty in the absolute age.

2.7 Air content age markers 0–440 kyr BP

The total air content of polar ice may be interpreted as a marker of the local summer insolation (Raynaud et al., 2007). Apparently, the solar radiative power absorbed at the surface influences the snow structure in the first upper meters and, in turn, the porosity of snow in the bubble close-off layer. The detailed physical mechanism is still under debate, however, the presence of a strong 41 kyr obliquity period in the air content signal makes it appropriate for the application of an orbital tuning method. We used 19 age markers from the air content age scale available back to 440 kyr BP. Each age marker corresponds to a minimum of obliquity, and the assumed uncertainty is 4 kyr^2.

2.8 $^{18}O_{atm}$ age markers for stages 300–800 kyr BP

A relationship between the isotopic composition of atmospheric oxygen ($\delta^{18}O$ of O_2, noted $\delta^{18}O_{atm}$) and daily northern hemisphere summer insolation has been observed at Vostok for the youngest four climate cycles. This property has been exploited to construct various orbital age scales for Vostok (Petit et al., 1999; Shackleton, 2000). Dreyfus et al. (2007) used a similar approach to derive an age scale for the bottom part of the EDC ice core (300–800 kyr BP) by assuming that $^{18}O_{atm}$ lags the summer-solstice precession variations by 5 kyr with an estimated uncertainty of 6 kyr. The selected age markers are placed at each mid-transition of $\delta^{18}O_{atm}$ (see Dreyfus et al., 2007, for more details).

2.9 The Brunhes-Matuyama reversal

The most recent of the geomagnetic inversions, referred to as the Brunhes-Matuyama reversal, has been localized between 3161 and 3170 m in the EDC ^{10}Be record (Raisbeck et al., 2006). This reversal has been dated radiometrically to have occurred 776±12 kyr BP (Coe et al., 2004), taking into account decay constant and calibration uncertainties. This transition has also been orbitally dated to be 778 kyr ago (Tauxe et al., 1996). Several authors have also reported evidence for a "precursor" event, 15 kyr before the B-M boundary (Brown et al., 2004), supported by the EDC ^{10}Be record.

Recently, the search for local insolation proxies in ice cores as, e.g. the O_2/N_2 ratio (Bender et al., 2002; Kawamura et al., 2007) or the air content record (Raynaud et al., 2007) has opened new prospects for eliminating the reliance on this hypothesis of constant insolation/climate phase, potentially allowing an accuracy within 1 kyr to be achieved in the coming years.

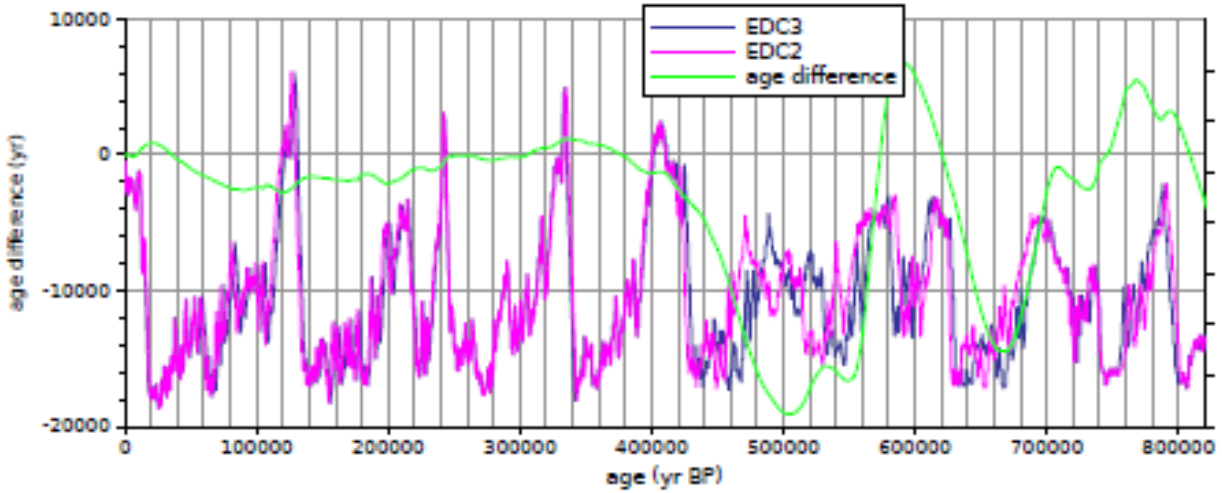

Fig. 2. Comparison of the EDC deuterium record on the EDC2 and EDC3 time scales. The green curve represents the difference in age between EDC2 and EDC3. Y-axes for isotopic records are normalised.

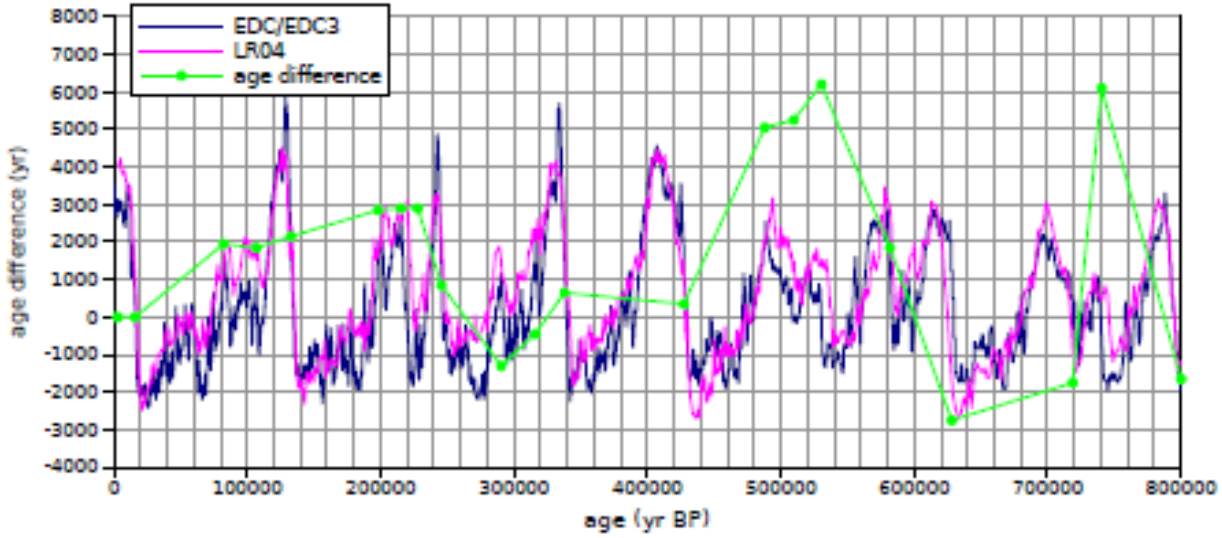

Fig. 3. Comparison of the EDC deuterium record on the EDC3 time scale with the LR04 marine stack on its own time scale, shifted by 3 kyr towards older ages. The green curve represents the difference in age between LR04 (+3 kyr) and EDC3 assuming both records are synchronous. Y-axes for isotopic records are normalised.

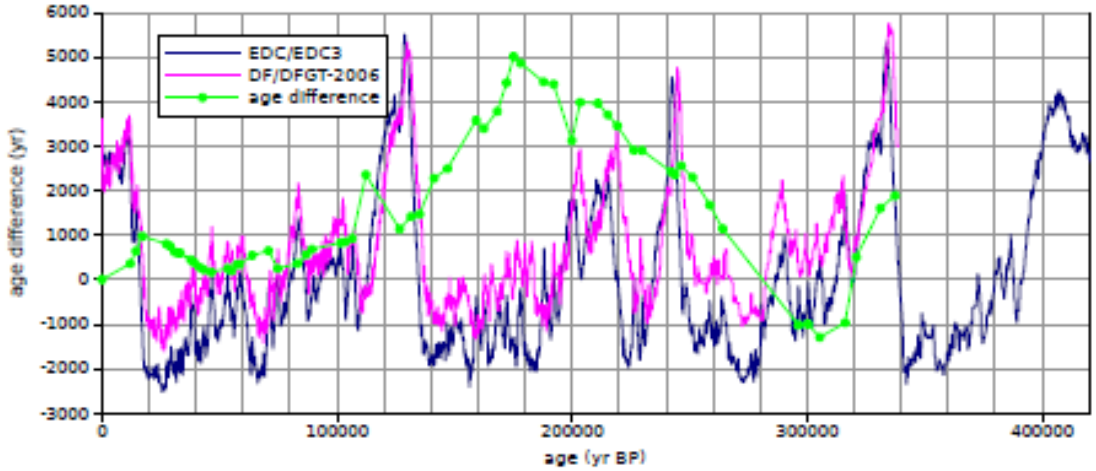

Fig. 4. Comparison of the EDC deuterium record on the EDC3 time scale with the Dome Fuji $\delta^{18}O$ record on the DFGT-2006 time scale (Parrenin et al., 2007). The green curve represents the difference in age between DFGT-2006 and EDC3 at the depth of the synchronisation markers. Y-axes for isotopic records are normalised.

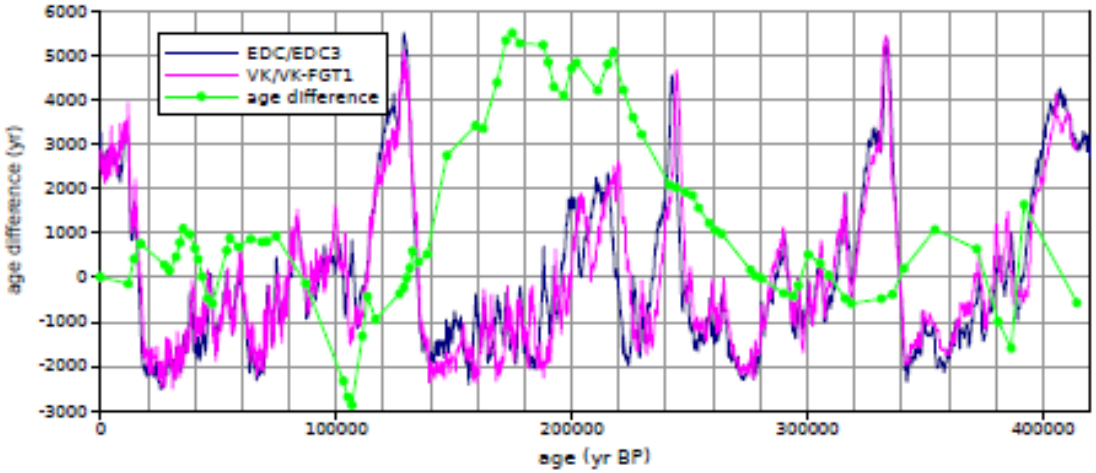

Fig. 5. Comparison of the EDC deuterium record on the EDC3 time scale with the Vostok deuterium record on the VK-FGT1 time scale (Parrenin et al., 2004). The green curve represents the difference in age between VK-FGT1 and EDC3 at the depth of the synchronisation markers. Y-axes for isotopic records are normalised.

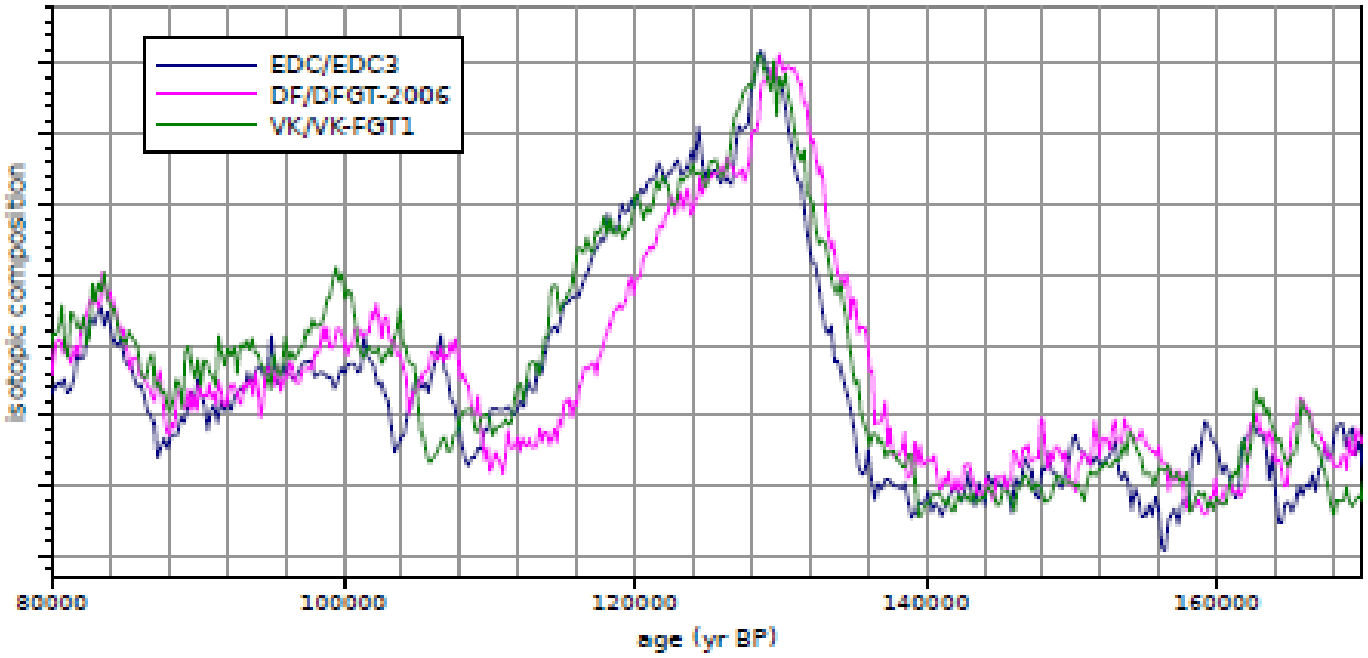

Fig. 6. Comparison of three glaciological age scales during the time interval MIS6-MIS5.4. The EDC deuterium record is on the EDC3 time scale. The Vostok deuterium record is on the VK-FGT1 time scale (Parrenin et al., 2004). The Dome Fuji $\delta^{18}O$ record is on the DFGT-2006 time scale (Parrenin et al., 2007). Y-axes for isotopic records are normalised.

Per saperne di più:

PROGETTO EPICA (European Project for Ice Coring in Antarctica): estrazione di una carota di 3200m di ghiaccio dal sito Dome C in Antartide che ha permesso tra le altre cose di ricostruire temperature e concentrazione dei gas serra negli ultimi 800 mila anni.

Alcune referenze:

- http://www.esf.org/index.php?id=855
- http://www.nature.com/nature/focus/epica/
- http://science.sciencemag.org/content/304/5677/1609.long
- http://science.sciencemag.org/content/310/5752/1317
- https://nsidc.org/data/nsidc-0244

http://www.nature.com/articles/srep20235https://en.wikipedia.org/wiki/European_Project_for_Ice_Coring_in_Antarctica

PROGETTO IPICS (International Partnerships in Ice Core Sciences): si tratta di un nuovo progetto in corso che dovrebbe spingersi oltre 1.5 milioni di anni fa nella ricostruzione del clima del passato tramite l'utilizzo di un carotiere di nuova concezione, di nome subglacior che permetterà di avere delle analisi in tempo reale, in situ grazie ad uno spettrometro montato nella sonda stessa.

- http://www.esf.org/hosting-experts/expert-boards-and-committees/polar-sciences/recent-epb-initiatives/europics.html
- http://www-liphy.ujf-grenoble.fr/-LAME-3A4-?lang=en
- http://www.igsoc.org:8080/annals/55/68/a68a026.pdf
http://polaris.nipr.ac.jp/~icc/NC/htdocs/?action=common_download_main&upload_id=35
- http://www.bgs.ac.uk/earthScienceEurope/downloads/EuropeanPartnership.pdf
- http://www.clim-past.net/9/2489/2013/cp-9-2489-2013.html
- http://scitation.aip.org/content/aip/journal/rsi/85/11/10.1063/1.4901018
https://www.researchgate.net/publication/268873097_Invited_Article_SUBGLACIOR_An_optical_analyzer_embedded_in_an_Antarctic_ice_probe_for_exploring_the_past_climate
- http://www.igsoc.org:8080/annals/55/68/a68a026.pdf
http://static1.squarespace.com/static/5459b25de4b00ee921cd006d/t/56c5125440261dc161e22a24/1455755861687/157-Catherine+Ritz.pdf
- http://www.nature.com/ngeo/journal/v6/n5/full/ngeo1797.html

PROGETTO ANDRILL: carotaggio nei sedimenti marini

Alcune referenze:
- http://www.andrill.org/static/index.html
- http://www.progettosmilla.it/2/andrill-il-progetto/

CAROTAGGI VOSTOK (lago sotterraneo nella zona della base russa)

Alcune referenze:
- http://www.nature.com/nature/journal/v399/n6735/abs/399429a0.html
- http://www.nature.com/nature/journal/v414/n6864/full/414603a.html
- http://www.nature.com/nature/journal/v399/n6735/full/399429a0.html

CAROTAGGI IN GENERALE
- http://www.antarcticglaciers.org/glaciers-and-climate/ice-cores/
- http://www.nature.com/nature/journal/v347/n6289/abs/347139a0.html
- http://onlinelibrary.wiley.com/doi/10.1029/96RG03527/full
- http://onlinelibrary.wiley.com/doi/10.1029/97JC01283/full
- http://www.sciencepoles.org/interview/climate-cycles-and-million-year-old-ice
- http://www.sciencepoles.org/article/frozen-grail-dome-a-and-the-future-of-ice-coring-in-antarctica